



GEM NEWS INTERNATIONAL

Contributing Editors

Gagan Choudhary, IIGJ-Research & Laboratories Centre, Jaipur, India (gagan.choudhary@iigirlc.org)

Christopher M. Breeding, GIA, Carlsbad (christopher.breeding@gia.edu)

Guanghai Shi, School of Gemmology, China University of Geosciences, Beijing (shigh@cugb.edu.cn)

TUCSON 2024

Overall, 2024 was a good year at the various Tucson shows. Foot traffic throughout the venues was noticeably slow at times, but less window-shopping and more serious buying of particularly higher-end items made up for the lack of bustling crowds. Most vendors interviewed reported strong sales and many returning buyers, noting that sales have continued to grow post-pandemic.

The American Gem Trade Association reported a small uptick in buyer attendance (+1%) and a 3% growth in vendors at the AGTA GemFair. In fact, they only had one empty booth in both the designer showroom and the gem hall. Vendors in both venues indicated that the show floor felt slower but that visitors were there to buy, often with shopping lists. AGTA's added security measures that included ID checks were well received by both buyers and exhibitors.

GIA's Show Service Laboratory reported a solid AGTA show, with ruby, emerald, and sapphire making up the majority of the intake. Both the service lab and vendors noted

Figure 1. A display case showing popular colors and materials seen this year in Tucson. Photo by Jennifer Stone-Sundberg; courtesy of Arizona Color Stones & Minerals.



Figure 2. Vintage turquoise rough from the Sleeping Beauty mine in Arizona. Photo by Jennifer Stone-Sundberg; courtesy of Arizona Color Stones & Minerals.

movement of high-end, unusual, and rare stones, a common theme every year in Tucson.

It was hard to miss the prevalence of green to blue stones, especially in vibrant and pastel tones. They were well represented in the 2023 AGTA Spectrum and Cutting Edge Awards, and many vendors reportedly brought these colors to Tucson in response. With blues and greens leading the way, pinks and to a lesser extent purples were also highly visible (figure 1). Among the top stones spotted throughout the shows were emerald, turquoise (figure 2), opal, aquamarine, Paraíba and cuprian tourmaline (figure

Editors' note: Interested contributors should send information and illustrations to Stuart Overlin at soverlin@gia.edu.

GEMS & GEMOLOGY, VOL. 60, NO. 1, pp. 90–138.

© 2024 Gemological Institute of America



Figure 3. A 30.26 ct blue cushion-cut cuprian tourmaline from Mozambique. Photo by Robert Weldon; courtesy of Evan Caplan.



Figure 4. A 5.34 ct vivid green modified cushion-cut Russian demantoid garnet displaying horsetail inclusions. Photo by Robert Weldon; courtesy of Tsarina Jewels.

3), green garnet (figure 4), and unheated Montana sapphire. Strong showings of unheated blue Ukrainian topaz, unheated bicolor green and blue zoisite, blue zircon, pink to purple garnets, electric pink and purple sapphire (figure 5), morganite, fluorescent "dragon" Malaya garnet, rose quartz, pink tourmaline, baroque pearls, and Oregon sunstone were also noted.

Another trend was the demand for visibly unheated stones. "Silky" sapphire and spinel with needle inclusions creating a soft, glowing appearance were extremely popular (figure 6). Also referred to as "opalescent," "hazy," "milky," and "sleepy," these stones were some of the hottest at the AGTA, Gem & Jewelry Exchange (GJX), and Pueblo shows. Dudley Blauwet Gems reported selling out of all of their opalescent milky stones by the fourth day of AGTA.

Other noted trends included the importance of geographic origin and traceability reporting for many buyers, the popularity of fancy shapes such as hearts and pears (figure 7), and the use of white metal in jewelry both in the AGTA Spectrum Award winners and throughout the shows.

Demand for American stones was evident once again, with more vendors carrying sapphire from Montana, turquoise from Nevada and Arizona, and sunstone from Oregon. In fact, one of the most often encountered materials in jewelry this year was vintage turquoise reportedly from the famed Sleeping Beauty mine in Arizona (figure 8). In the past, these various American gems were available mainly from vendors directly associated with the mining claims. The Southwestern motif, always a fixture in Tucson, was decidedly more pronounced this year, with many large silver items throughout the shows, including bangles, cuff



Figure 5. Pink and purple "Nebula" sapphire in both freeform faceted tablet (left; 7.77 × 9.20 mm, 0.82 ct) and brilliant-cut (right; 4 mm round, 0.73 ct) styles. This material is from a mine in Madagascar that produces very small stones ranging from hot pink to violet. Photos by Kalim Korey; courtesy of Caroline C.

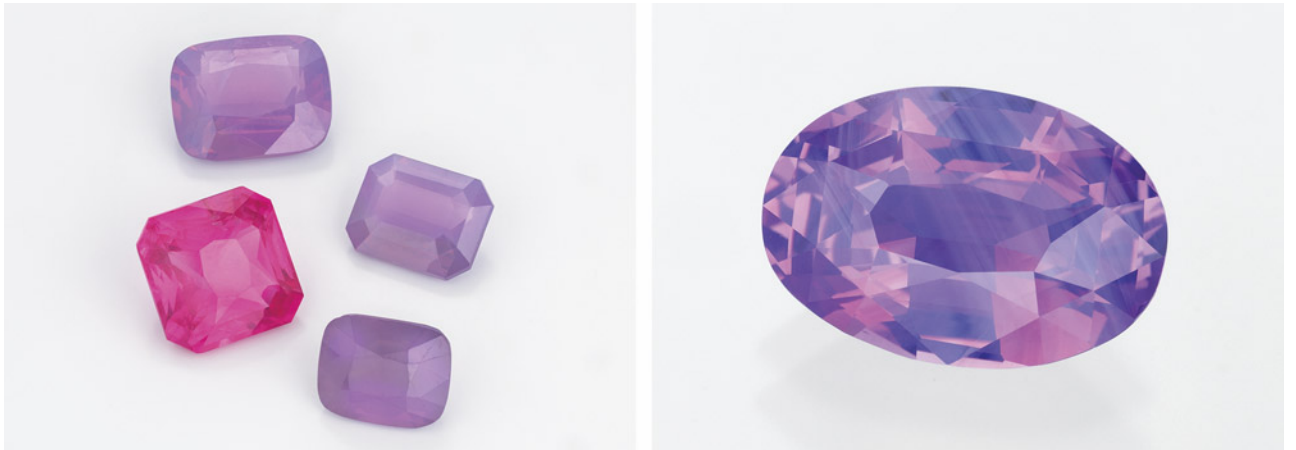


Figure 6. Sapphire and spinel with a visible silvery haze creating a glowing, sleepy appearance were popular throughout the shows. Left: Four emerald-cut Mahenge spinel (clockwise from top: 3.00 ct purple, 1.77 ct purple, 2.40 ct purple, and 3.71 ct hot pink). Courtesy of Bryan Lichtenstein. Right: A 4.50 ct “opalescent” unheated sapphire from Sri Lanka. Courtesy of Misfit Diamonds. Photos by Robert Weldon.

bracelets, statement earrings, necklaces, and bolo ties adorned with turquoise (figure 9), red coral, blue topaz, and opal. This observation was validated the following week when singer Post Malone performed “America the Beautiful” before Super Bowl LVIII wearing a striking silver bolo tie complete with a large bright green turquoise stone with brown matrix. The bolo was reportedly made by Navajo artist Leonard Nez of New Mexico using a piece of Royston turquoise.

In addition to the presence of vintage jewelry this year, we also found multiple examples of repurposing antiquities into jewelry. As for new finds, we report on bright blue opal from Chile, green amber from Ethiopia, high-quality

orange-flash rainbow moonstone from Madagascar, and recent sapphire production from the famed Kashmir region.

We hope you enjoy our coverage of the 2024 Tucson gem shows and find the following reports informative.

*Jennifer Stone-Sundberg, Tao Hsu, Eric Fritz,
Lisa Kennedy, and Cristiano Brigida*

Figure 7. A 0.67 ct heart-shaped pezzottaite measuring 5.61 × 6.10 mm. The rough of this rare newer gem material was found and bought in Madagascar in December 2023. The stone was cut in New York for the Tucson show, where it sold. Photo by Kalim Corey; courtesy of Caroline C.



Figure 8. Two pairs of earrings designed and crafted by Caroline Chartouni using Sleeping Beauty turquoise rough she acquired more than 10 years ago. The left pair is 18K white gold with 64.53 carats of turquoise, two cabochon moonstones, and 4.40 carats of hot pink spinel. The right pair is 18K white gold with 107.30 carats of turquoise, 4.64 carats of tsavorite garnet, and 0.19 carats of diamond. Photos by Kalim Corey; courtesy of Caroline C.





Figure 9. Vintage Navajo silver bolo tie with turquoise reportedly from the Morenci mine in southeastern Arizona, which is not currently being mined for turquoise. This highly collectible material, known for its desirable blue color and iron pyrite matrix, dates back to 1864 and was a byproduct of copper mining. Photo by Kevin Schumacher; courtesy of Aaron Palke.



Figure 10. This clean piece of tumbled green amber from Ethiopia, measuring approximately $5.5\text{--}6.0 \times 2.8\text{--}3.5$ cm, displays flow structures and some inclusions. Photo by Cristiano Brigida; courtesy of Rainbow King Solomon Mines.

COLORED STONES AND ORGANIC MATERIALS

Green amber from Ethiopia. Many consumers and gem enthusiasts are most familiar with yellow and golden amber commonly found in the Baltic Sea region and the Dominican Republic. However, the gem can also be white, orange to red, or brown. In rare cases, strong fluorescence can give amber a bluish or greenish appearance.

At the Pueblo Gem & Mineral Show, Rainbow King Solomon Mines showed the authors some rare green amber said to be from the Amhara region of Ethiopia. The selec-

Figure 11. Ethiopian faceted green amber, measuring approximately 18×18 mm. The gem looks very lively under sunlight. Photo by Cristiano Brigida; courtesy of Rainbow King Solomon Mines.



tion consisted mainly of large tumbled pieces with a yellowish green to greenish yellow bodycolor, visible flow structure and bubbles, moderate to heavy inclusions, and numerous brown discolorations (figure 10). A few pieces contained sizable insect inclusions as well. The exhibitor presented a limited amount of experimental faceted pieces (figure 11), but these were not for sale. The faceted pieces showed a surprisingly high luster and brilliance, as well as fiery flashes of orange and green colors. Because of the material's dark tone, prominent brown discolorations, and relative abundance of biological inclusions—no samples were tested by the GIA laboratory—the authors believe it was natural, compared to the green autoclaved copal previously described by Abduriyim et al. ("Characterization of 'green amber' with infrared and nuclear magnetic resonance spectroscopy," Fall 2009 *G&G*, pp. 158–177).

The discovery of Ethiopian amber deposits is relatively recent, with orange to yellow amber most commonly found. Compared to other amber sources, the occurrence of green amber in Ethiopia is more prevalent but still rare overall and limited to certain localities. The amber observed at the Pueblo show matches the characteristics of the highly bio-included green amber described in detail by Bouju and Perrichot ("A review of amber and copal occurrences in Africa and their paleontological significance," *BSGF - Earth Sciences Bulletin*, Vol. 191, 2020, article no. 17).

Lisa Kennedy and Cristiano Brigida
GIA, New York

An exceptional cat's-eye emerald. Those in the gem trade often recall a memorable experience, gemstone, or business connection. A Brazilian cat's-eye emerald (figure 12) presented at the AGTA show by estate dealer Doug Liebman (Scottsdale, Arizona) conjured all three.

Figure 12. Double cabochon cat's-eye emerald weighing 5.11 ct and measuring $10.77 \times 8.95 \times 7.39$ mm, from Goiás State, Brazil. Photo by Robert Weldon; courtesy of Douglas M. Liebman Estate Jeweler.

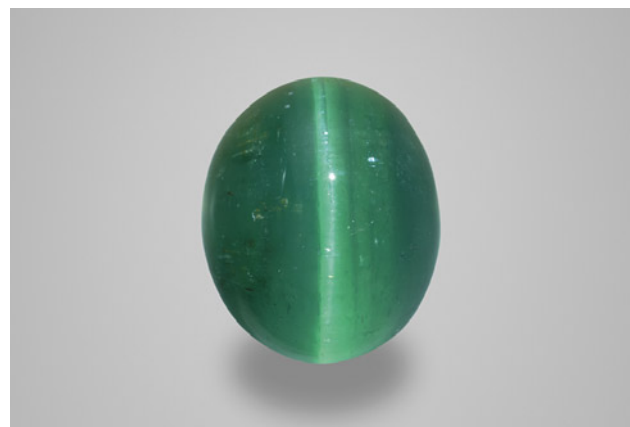




Figure 13. Left: "Meteorites," a mosaic by Leonardo Scarpelli. A labradorite background gives a strong sense of light shining in the night sky as the observer moves. Right: The "Starburst" mosaic by Leonardo Scarpelli. Larimar proved the perfect material to reproduce aquamarine's transparency and color. Photos by Cristiano Brigida; courtesy of Scarpelli Mosaici.

Liebman shared the story of how in 1983, early in his career, he forged a long-term relationship with Albert Sabbagh, cofounder of Ben Sabbagh Bros. in Brazil. Liebman's early buying trips to Brazil revealed a wide variety of gemstone offers at all price points, including the magnificent cat's-eye emerald.

Emeralds have been mined sporadically and in small quantities in the Brazilian state of Goiás for more than 100 years. In 1981, the deposits were found to produce emerald of a desirable quality. This prompted more steady mining, which has been continuous ever since. The emeralds occur in a talc schist as stubby crystals usually less than 1 cm long. Their color ranges from pale to dark green, often with a bluish overtone. The best faceted stones are rarely over one carat.

Last year, at GJX 2023, Liebman visited the Ben Sabbagh Bros. booth and spoke with Albert's sons Samuel and Clement. They showed him a cat's-eye emerald from Goiás that had been part of their late father's private collection. Liebman recalled the emerald from his early days with Sabbagh. While impressed by the stone, he left the booth without buying.

After some reflection, Liebman returned to GJX first thing the next morning. He said yes to the emerald before they even told him the price.

The 5.11 ct cat's-eye emerald is extraordinary for its color, clarity, legacy, and allure, with no additional light source needed to display the centerline cat's-eye effect. What goes around often does come back around, at the right time, in the right place: Tucson, Arizona.

Eric Fritz
GIA, Carlsbad

Gemstones and art. Exploring the Tucson Fine Mineral Gallery, the author was impressed by artistic masterpieces hanging from the walls. These exhibits ranged from stone

mosaics of modern subjects to watercolor paintings of minerals. The author had the chance to speak with mosaic artists Leonardo and Catia Scarpelli (Scarpelli Mosaici, Florence) and watercolor artist Ksenia Levterova (Kyiv).

The Scarpelli family creates stunning mosaics representing contemporary subjects using the technique of *commesso fiorentino* (from the Latin *commettere*, meaning "put together"), which dates back to the Italian Renaissance. In this craft, opaque stones of different colors and textures (*pietra dura*) are finely cut into unique shapes and seamlessly joined together. This traditional art form developed and achieved a level of perfection in the late sixteenth century in Florence, under the rule of the Medici family, who wanted to depict their era in a durable, eternal medium.

Leonardo Scarpelli, the son of a *commesso fiorentino* master, began his career in 1992. Challenged by the idea of moving from traditional to more modern subjects, he experimented with the *commesso fiorentino* technique by incorporating gem materials that had never been used before, such as labradorite. Scarpelli discovered that labradorite brought depth and life to subjects where dynamism is essential, such as a splashing water drop or meteorites falling in the night sky (figure 13, left), allowing him to create unusual motion effects unexpected from a traditional mosaic.

After Scarpelli exhibited in some gem and mineral shows, the idea of reproducing mineral specimens with the proper transparency and color nuances by means of *commesso fiorentino* became a compelling challenge. When commissioned to reproduce a fine aquamarine specimen from Pakistan, the Scarpellis' extensive search for the right color landed on Larimar, the trade name for a variety of pectolite. Its light blue color and white speckles made Larimar ideal for the purpose, leading to impressive results (figure 13, right). This is one more case where the use of a gem material associated with traditional stones demonstrated all its potential in bringing into play precious effects, colors, and textures.

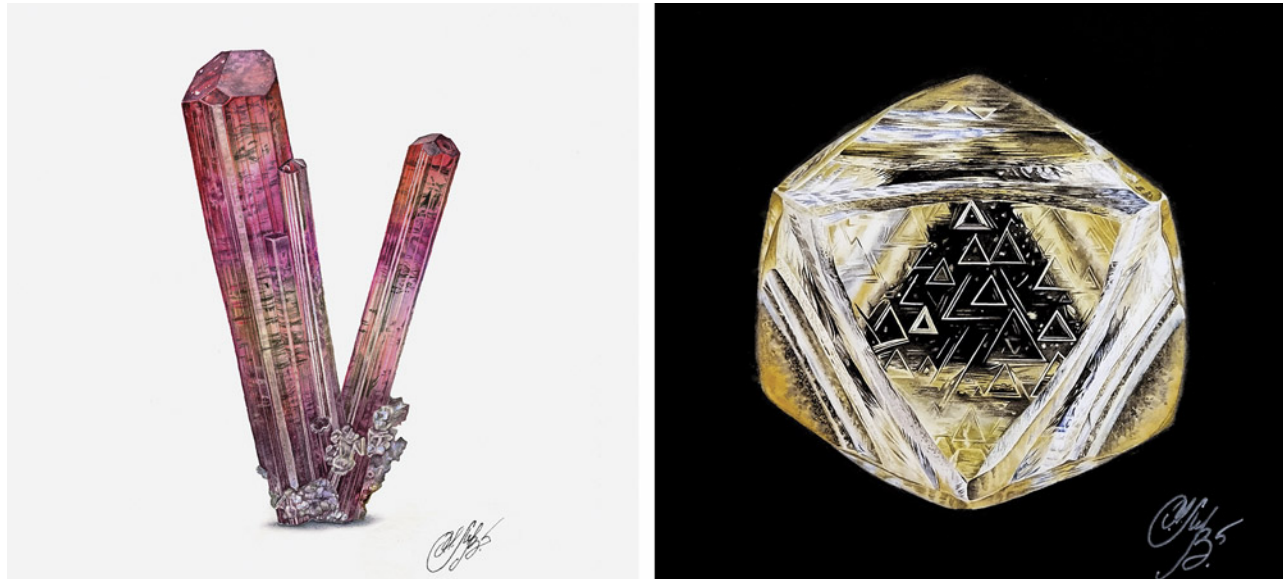


Figure 14. Watercolors of tourmaline with albite (left) and a diamond crystal from Kimberley, South Africa (right). Photos by Cristiano Brigida; courtesy of Ksenia Levterova.

Ksenia Levterova is a talented Ukrainian watercolor artist. Passionate about the perfection of mineral shapes and their fascinating colors, she specializes in the reproduction of mineralogical subjects at a photorealistic level.

Levterova's artworks exhibited in Tucson this year encompassed a wide range of subjects, from the captivating beauty of fine specimens such as tourmaline to the precise reproduction of mineral crystallizations (figure 14). Watercolor makes it possible to represent the most subtle variations in color and transparency effects while displaying each crystal's characteristics with remarkably high definition. The degree of realism and the fidelity to shapes and color nuances allow a rigorous mineralogical consistency. As a result, Levterova's work is becoming popular in many gem and mineral shows, and she has a gallery hosted on Mindat (<https://www.mindat.org/gallery-63606.html>).

Cristiano Brigida

Butterfly brooch showcasing East African gems. At the AGTA show, Andrew Rosenblatt, company spokesperson for Akiva Gil (New York City), showed us a magnificent butterfly brooch featuring colored stones from East Africa (figure 15). Notably, Akiva Gil was among the first to acquire spinel and raspberry rhodolite from Tanzania in the early 2000s. Joseph Gil collaborated with the late master jeweler

Pietro DiBenedetto to develop a piece that would showcase the beautiful array of colors from this part of the world.



Figure 15. This colorful 18K gold butterfly brooch designed by Pietro DiBenedetto features 49 East African colored gems, accompanied by colorless and yellow diamonds. Photo by Robert Weldon; courtesy of Akiva Gil & Co.

The resulting brooch contains fine-quality green tsavorite (17.98 carats total), yellow grossular (0.98 carats total), and orange mandarin garnets (10.15 carats total) alongside pink spinel (15.00 carats total) and fancy-color sapphire (8.47 carats total). These are accented by 1.60 carats of yellow and colorless diamonds. This piece highlights the wide range of colored gem varieties in highly desirable hues that East Africa contributes to the gem trade today.

*Jennifer Stone-Sundberg and Robert Weldon
GIA, Carlsbad*

Guatemalan jadeite jade: Rough and finished. Jadeite jade is one of the most important aggregate gems in today's global marketplace, with known sources in Myanmar, Japan, Russia, and Guatemala. Among them, Myanmar is the most legendary and still dominates today's market. Guatemala, however, has recently reclaimed its status as an important jadeite jade producer (see Z. Huang et al., "Ice jade' from Guatemala," pp. 26–41 of this issue).

At this year's 22nd Street show, Yax Tun Minerals (Denver, Colorado) offered a wide range of Guatemalan jadeite jade, including rough pieces in blue, green, and lavender (figure 16). According to owner Luke Miller, the bluish color is the most common and the most desired in the American market. All rough is covered with a "skin" resulting from weathering.

The seller provided a strong flashlight for buyers to assess the quality of the rough, similar to what buyers do at the major jadeite auction in Myanmar. The blue color was quite saturated, while the green and lavender colors were not. The bluish rough showed high transparency and some had green veins running through it (figure 17, left). The green veins also exhibited high transparency (figure 17, right). The lavender rough pieces were of low transparency



Figure 16. The rough Guatemalan jadeite jade sold by Yax Tun Minerals included blue, green, and lavender hues, with blue being the most prevalent. Photo by Tao Hsu; courtesy of Yax Tun Minerals.

and had a coarser texture than the other two color varieties (figure 16).

The blue color is characteristic of Guatemalan jadeite jade, which is often called "Olmec blue" in the trade. The Olmec civilization was a Mesoamerican culture revealed by archaeological artifacts. The blue to green-blue jadeite jade mined in Guatemala was prized by the Olmecs from about 1500 to 400 BCE. Mesoamerican cultures that fol-



Figure 17. The bluish jadeite jade from Guatemala showed high transparency and a very fine texture (left). Some displayed green veins throughout. A flashlight revealed a slight green tint in some pieces with high transparency and fine texture (right). Photos by Tao Hsu; courtesy of Yax Tun Minerals.



Figure 18. This spectacular “Rainbow Luna” dagger features a blade of beautiful Guatemalan jadeite jade that shows the characteristic Olmec blue color and even deeper purplish blue close to the point. Courtesy of Georg Schmerholz.



Figure 19. An 18K yellow gold and blackened sterling silver shagreen wide cuff bracelet, pendant, earrings, and ring set with antique mother-of-pearl gaming counters. Courtesy of Sarosi by Timeless Gems.

lowed, such as Mayan, Zapotec, and Totonac, continued the reverence for jadeite jade. But when the Spanish conquered Mesoamerica in the sixteenth century, their appetite for gold and emeralds contributed to the fall of Guatemalan jadeite jade popularity. Mayan guards kept the jade mine locations secret, and they were not rediscovered until 1974. Since then, Guatemala has been gradually regaining recognition as an important source of jadeite jade.

Finished products offered at the Yax Tun booth included beads, beaded necklaces, bracelets, earrings, and small pendants, polished or carved. Many of the top-quality materials are processed at Miller's carving studio in Mexico.

As Guatemalan jadeite jade gains popularity among both Western and Asian consumers, more gem artists are using this material to show their creativity. World-renowned sculptor Georg Schmerholz brought an outstanding collection of jade to the Tucson Gem and Mineral Show. His latest creation, "Rainbow Luna," is second in the "Resplendent Quetzal" series, which honors a beautiful bird native to Guatemala. Completed in June 2023, the 14-inch dagger is carved from the finest Guatemalan jadeite jade with a patinated bronze handle (figure 18). Schmerholz's jade art bridges the two disciplines of sculpture and gemstone carving.

The wide range of appearance and quality of Guatemalan jadeite jade offers versatility to designers, artists, and consumers. Sufficient production and distribution are essential for this gem material to reach a wider audience.

Tao Hsu
GIA, Carlsbad

Historical relics repurposed into jewelry. One theme that emerged at the AGTA, GJX, and Pueblo shows was the repurposing of historical artifacts to produce new jewelry items. We saw the incorporation of Chinese, Greek, Viking, and medieval European artifacts into various jewelry pieces at all three shows. Many attendees were drawn to the idea of having a connection to the past in a wearable form.

At GJX, Sarosi by Timeless Gems (Los Angeles) exhibited eye-catching carved mother-of-pearl jewelry (figure 19). While the sheer beauty of the pieces initially caught the authors' attention, the craftsmanship and story behind them enabled this collection to stand out among a sea of designs. At the center of all the pieces in the collection were hand-engraved mother-of-pearl Chinese gaming counters, once used like modern-day gambling chips. The eighteenth-century counters were commissioned by British royalty and nobility during the Qing Dynasty. Most were engraved on one side with family crests or monograms, with the reverse side illustrating some aspect of Chinese life. The counters were surrounded by a combination of 18K yellow gold, polished sterling silver, and blackened sterling silver, handcrafted by jewelers in Los Angeles to evoke traditional Chinese architecture.

In the AGTA designer showroom, Zaffiro (Walla Walla, Washington) devoted a section of their case to their artifact collection, comprising sixth- to fifteenth-century Viking, Anglo-Saxon, and European medieval relics that they incorporated into jewelry (figure 20). These one-of-a-kind pendants integrate actual buried treasure purchased from a reputable auction house in the UK. Zaffiro founders Jack and Elizabeth Gualtieri explained that they



Figure 20. Three ancient artifacts repurposed by Zaffiro. Top left: Medieval silver-gilt strap end from the thirteenth to fifteenth century, set in granulated 22K yellow gold with a 0.07 ct red spinel. Center: Gilded bronze medieval mount from the twelfth to fourteenth century, set in 22K granulated and 18K yellow gold with 0.15 carats of tsavorite garnet and an 11.5 x 14.0 mm black Tahitian pearl. Bottom right: Gilded bronze belt mount from the tenth to twelfth century, set in granulated 22K yellow gold with a 0.13 ct blue sapphire. Photo by Robert Weldon; courtesy of Zaffiro.

like to use items from before the advent of the printing press. Many of the antiquities, originally used to decorate items such as belts, clothing, and horse tack, have retained their original gilding. The Gualtieris set the artifacts in 22K gold frames or rivets and decorate with granulation, sometimes accenting the pieces with colored stones. The appeal of these pieces is in the stories that they tell.

Back at the GJX show, Shans Premier (New York City) offered a large selection of antiquities, including coins in addition to colored stones and jewelry. This multi-generational business has been dealing in antiquities for more than 100 years and in the U.S. for about 40 years. This was their thirtieth year in Tucson. They typically sell more gemstones at

U.S. shows, but in Tucson they have a strong following for their antiquities.

Sason Shan described a particularly intriguing pendant incorporating one of the most circulated coins from the height of classical Greek civilization: the silver Athenian owl tetradrachm (figure 21). This surprisingly heavy coin was used throughout the ancient world around the time of the Peloponnesian War. Greece minted enormous quantities of these coins using silver from Laurion. Worth several days' wages, they were too valuable for basic transactions (R.A. Augustin, "Ancient coins – The most famous coin of antiquity – The Athenian owl," *Coin Week*, 2022, accessed February 10, 2024, <https://coinweek.com/ancient-coins-famous-coin-antiquity/>).



Figure 21. A silver Greek Athenian owl tetradrachm from the fifth century BCE weighing approximately 17.2 g with an approximate diameter of 24 mm set in an 18K yellow gold pendant, which cleverly allows the rotation of this coin to face upward on both sides even though the two sides are not stamped in the same orientation. The left image shows the coin obverse with a profile of Athena, and the right image shows the coin tail featuring her patron animal, the owl, which was also a symbol of ancient Athens. Photos by Jennifer Stone-Sundberg; courtesy of Shans Premier.

With sustainability at the forefront of many consumers' minds, these upcycled designs extend the life of antiquities, allowing them to be displayed for many years to come.

Lisa Kennedy and Jennifer Stone-Sundberg

Intarsia jewelry box by Nicolai Medvedev and Susan Helmich. Opening day at the AGTA show was truly memorable with the premiere of "Treasure Chest II with Blue Boy" (figure 22, left), a joint collaboration between intarsia

master Nicolai Medvedev and jewelry designer Susan Helmich. The exterior of the chest is adorned with Australian opal, Paraíba tourmaline from Brazil, diamonds, South African sugilite, Burmese maw-sit-sit, turquoise from the Sleeping Beauty mine (Arizona) and Nevada, gold-in-quartz from Australia and California, Utah dinosaur bone, 22K gold, and a matched pair of exquisite opal slices from Virgin Valley, Nevada. This type of Nevada opal is commonly referred to as "conk" wood, in which the cells of the original wood have been opalized. The slices featured

Figure 22. Left: The front of the "Blue Boy" chest features two wing-like "conk" wood opal slices from Nevada. Right: A 22K gold stingray adorns the top of the chest, guarding the contents within. Photo by Robert Weldon.



on the front of the box came from the Bonhams opal and phenomenal gem auction in 2021.

The stingray "Blue Boy" on top was designed and hand carved by Helmich, created from 22K gold with Paraíba tourmaline and diamonds (figure 22, right). The interior is lined with burl wood veneer, with jasper inset into the lid, malachite (Bisbee, Arizona), and an 18K gold hinge. The chest, which took two years to complete, is the second in the series from Medvedev and Helmich. Their first chest featured an octopus.

Eric Fritz

New high-quality rainbow moonstone from Madagascar. Moonstone, a perennial favorite in Tucson, was offered both as loose stones and in jewelry throughout the shows. This year, a new type of transparent moonstone from Andilamena in the Alaotra-Mangoro region of northeastern Madagascar displayed a distinct orange flash effect in addition to strong blue adularescence. Moonstone is normally cut en cabochon, but the two moonstones in figure 23 were faceted because of their high transparency and to better display the orange flash.

Blue moonstone is a phenomenal gemstone variety of orthoclase, a mineral belonging to the alkali feldspar group. This potassium aluminum silicate gem is transparent to translucent, with a white bodycolor and blue adularescence. The blue "moonlight" is caused by light interference from moonstone's alternating microscopic layers of albite and orthoclase. Rainbow moonstone, which shows flashes of various colors that can include blue, is also a feldspar mineral but belongs to the plagioclase group and falls into the calcium-rich labradorite variety. This new material was confirmed to be plagioclase feldspar and within the labradorite variety by Bear Williams (Stone Group Lab-



Figure 23. A 9.30 ct oval cut and a 4.12 ct triangular cut of a new type of moonstone from Madagascar featuring an orange flash effect. Photo by Robert Weldon; courtesy of Dudley Blauwet Gems.

oratories, Jefferson City, Missouri) using Raman spectroscopy, making this a high-quality rainbow moonstone.

This new material was reportedly mined in 2023, and the initial supply of several kilograms of rough sold out at extraordinarily high per-carat prices. Hopefully more of this intriguing material will reach the marketplace soon.

Jennifer Stone-Sundberg

Morganite from Blue Star Gems. Morganite, a pink gem discovered in 1910 in Madagascar, was identified as a new variety of beryl by George Kunz, who named it in honor of his friend J.P. Morgan. Morganite has since been found in several other countries, most notably Brazil, Mozambique, Afghanistan, China, Russia, and the United States. The most productive mine today is in Minas Gerais, Brazil.



Figure 24. The 236.27 ct pear-shaped untreated morganite from old Madagascar stock was designed by Prakash Chand Vijay, who also oversaw the cutting. Photos by Jennifer Stone-Sundberg (left) and Robert Weldon (right). Courtesy of Blue Star Gems.

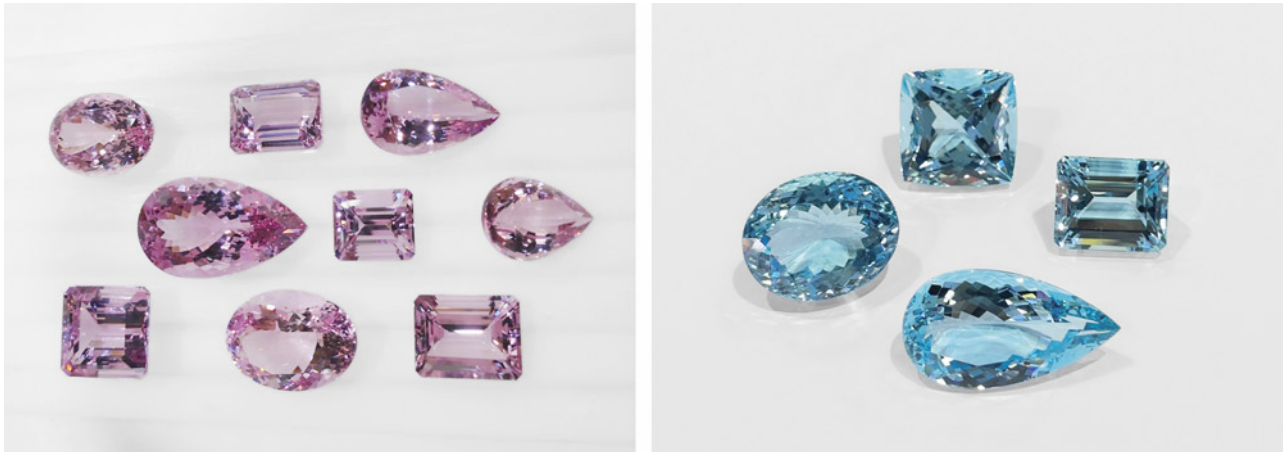


Figure 25. Left: Suite of morganite from Mozambique ranging from 27.90 ct (the center rectangular step cut) to 92.34 ct (the largest pear). These stones underwent a lengthy heating and electron radiation treatment to bring out the best color and clarity. Right: Suite of aquamarines from Madagascar. Clockwise from left: 31.88 ct oval brilliant cut, 49.08 ct cushion cut, 35.80 ct rectangular step cut, and 24.51 ct pear brilliant cut. Photos by Prateek Vijay; courtesy of Blue Star Gems.

At the GJX show, an extraordinary morganite stood out at the Blue Star Gems (New York City) booth (figure 24). Owner Prakash Chand Vijay indicated that the 236.27 ct stone was from vintage stock from the original morganite mine in Madagascar. This one-of-a-kind untreated stone had a particularly pleasing deep warm pink color and a striking constellation of small inclusions scattered throughout. With Vijay's expertise in the selection and cutting of stones from Africa, he participated in and oversaw the cutting of this exceptional gem.

Vijay's daughter, Jyoti Vijaywargi, said that this year they brought more than 100 pieces of attractively colored purplish pink morganite in sizes of over 20 carats each (figure 25, left). These stones came from Mozambique and underwent a lengthy heating and electron irradiation treatment in Germany to bring out the best color and clarity.

The enhancement of morganite color has been shifting from neutron irradiation to electron irradiation, avoiding the risk of a radioactive product (T. Stephan et al., "Irradiation treatment and gamma-ray spectroscopy of morganite," *37th International Gemmological Conference Proceedings*, Tokyo, 2023, pp. 123–125). Vijaywargi noted that due to the large sizes of their morganites, the entire process takes about five years to produce the quality seen, attesting to the value of the material and the patience of the vendor. The treatment itself takes about three and a half years, followed by an additional 18 months to let the stones cool down and be tested before they can be sold. Sometimes the stones do not respond to the treatment, and there is no color improvement at all. To date, there is no pretreatment testing to indicate whether the stones will respond to the treatment, so each run is a financial risk.

In addition to morganite, Blue Star Gems had extensive offerings of aquamarine (figure 25, right)—one of this year's

most popular stones—and tanzanite. The aquamarine comes from Madagascar. Despite global business challenges, the show proved successful for Blue Star Gems, particularly for high-end stones. The company was also able to attract new buyers this year.

Vijaywargi described the recent challenges around the pricing of wholesale versus retail items. On the wholesale side, prices for all goods have increased, yet these price changes have not been reflected at the retail end. As a vendor carrying substantial inventory of rare gemstones, Vijaywargi anticipates an increase in the value of Blue Star's collection, which will require patience as a seller.

Jennifer Stone-Sundberg

Blue opal from Chile. Opal is an extremely popular stone in its many phenomenal varieties. However, the market also offers countless types of nonphenomenal opal, whose selling point is their combination of color, pattern, and degree of transparency.

At the 22nd Street show, the author came across an enchanting ocean blue variety of opal from Chile, exhibited by Chilean Rocks and Minerals. The material on view was opaque to semitranslucent with an overall color banding and greasy luster, tumbled or cut as cabochons. The most prized pieces contained slightly greenish and vivid blue colors (figure 26, left). Less valuable polished stones showed alternating blue and solid white layers or the presence of green material and sometimes brown matrix in their bands. The cutters used the natural banding to their advantage, resulting in attractive colors and patterns that often evoke pleasant seascapes (figure 26, right). After cutting, the material is polymer impregnated to create a tough and durable finished product.



Figure 26. Left: A polished Chilean blue opal pear-shaped cabochon displaying a uniform and strongly saturated medium blue color and a greasy luster. Right: An oval cabochon representative of the typical color palette and banding, varying from bluish green to slightly greenish blue and pure white, which produces a "seascape" image. Photos by Cristiano Brigida; courtesy of Chilean Rocks and Minerals.

A selection of various grades of rough material was also available, displaying a dull conchoidal fracture with the dominant textural feature being the intricate interplay of blue and green, the two main colors (figure 27).

According to the dealer, this was the debut of cut Chilean blue opal at the Tucson gem shows. This type of opal is reportedly from the Atacama region, the only known occurrence to date in Chile, where a few mining operations are actively extracting the material. Presently known to the trade is a blue opal from Peru referred to as "Andean opal," but that material is generally translucent and lower in saturation than the Chilean blue opal.

No detailed mineralogical analyses on the samples exhibited at 22nd Street have been reported. The blue color could be due to internal light scattering and dispersed chrysocolla, a mineral known for its vivid blue hue. Chrysocolla is commonly found in copper-rich deposits such as the porphyry copper deposits in the Atacama region. The analogy with Peruvian blue opal, which comes

from a similar chrysocolla-rich geological setting, supports this hypothesis.

Given its vibrant color saturation, ability to take a high polish, and the desirable texture and alternating color patterns of the cut stones, this Chilean blue opal was a pleasant new addition to the gem offerings from Tucson 2024.

Cristiano Brigida

Precious opal from Pedro II, Brazil. Prime Gems, Inc. (New York City) offered a small quantity of precious opal from Brazil at this year's GJX show. As an opal source, Brazil has been underrepresented for the past four decades since a "golden age" from the 1960s to mid-1970s. The inventory of Brazilian opal from Prime Gems helped inform attendees of the fine quality available from this part of the world.

Multiple states in Brazil have opal occurrences, but the most important reserves are in the Pedro II munici-



Figure 27. Rough sample of Chilean blue opal, about 18 cm wide, displaying a dull conchoidal fracture, alternating green and blue bands, some white lenses (milky quartz), and a light brown matrix. Photo by Cristiano Brigida; courtesy of Chilean Rocks and Minerals.



Figure 28. Pedro II is the most important opal source in Brazil. The town is located in the northeast of the state of Piauí, and opal deposits are distributed in an area about 20 km in diameter around the township. The current opal mine is an open-pit operation. Photo courtesy of Prime Gems.

pality, located in the northeastern state of Piauí (figure 28). According to the local artisanal miners, the first precious opals were found near the end of the 1930s. During its peak in the 1960s and 1970s, more than 30 mining operations were active. However, by the early 1980s, over two-thirds of the mines were abandoned. Currently, opal mining in this area is still small-scale and mostly manual.

The opals in this region are found in both primary and alluvial deposits. In the primary deposits, opal occurs in

veins in the host sandstones (figure 29, left). This occurrence is similar to Australian opal deposits in that both are of a sedimentary nature. The vendor displayed an interesting rough opal attached to a piece of intrusive igneous rock, creating a "salt and pepper" appearance (figure 29, right). According to the vendor, diabase dikes intruded into the sedimentary rocks in this area. Diabase is of basaltic composition, and its main constituent minerals are plagioclase feldspar and pyroxene, which are of lighter and darker colors, respectively. This rough piece shows that opal also develops

Figure 29. Opal rough from Pedro II shows that opal can occur in veins in the host sedimentary rocks (left) or as thin layers attached to intrusive dikes (right). The sedimentary rocks have a light color, while the dikes are darker. Photos by Tao Hsu (left) and Robert Weldon (right); courtesy of Prime Gems.





Figure 30. High-quality opal from Brazil shows extremely vivid play-of-color. Some are of transparent light gray to white bodycolor such as this 132.3 ct freeform (left), while others have darker bodycolor (right). Photos by Robert Weldon; courtesy of Prime Gems.

at the contact between the dike and the host sedimentary rocks.

At the region's alluvial deposits, miners wash and manually extract opal. This is hard work but feasible for those who cannot afford mechanical equipment. Most of the miners alternate between opal mining during the dry summer and farming in the rainy season.

Prime Gems offered Brazilian opal with transparent light gray to white bodycolor from Pedro II, similar in appearance to white opal from Australia (figure 30, left). The play-of-color was especially charming in less transparent pieces that showed colors of the whole spectrum, with bluish and greenish colors most commonly displayed. Red play-of-color is rarer and more sought after, with a higher price tag. Some pieces with darker bodycolor resembled Australian black opal (figure 30, right).

Finished products available at the show included loose opal as cabochons, freeform polished singles or pairs, doublets, and some mosaic pieces. The top-quality materials displayed a vibrant whole-spectrum play-of-color. Opal that was of good quality but too thin for freeform single pieces was used to make doublets, with the thin opal layer glued to a dark base. To support local communities, mine operators allow the local people to use very small pieces of opal from mine waste to create mosaics for sale. The supplemental income from the sales of the mosaics can reach as much as \$30 per day.

The miners informed the author that Brazilian opals are sometimes sold as Australian in the marketplace. Brazilians are proud of the quality of their opal, and opal from Pedro II is one of the two products from the state of Piauí that bear the Geographical Indication certificate. The Brazilian government grants this GI label to products or services that are characteristic of a region. The aim is to ensure that Brazilian opal is properly represented and can generate revenue to further support mining and the local communities.

Tao Hsu

Patania Jewelry. At the GJX show, the Patania Jewelry booth featured striking silver jewelry, incorporating turquoise, red coral, and other gems, that stood out for its diversity in style. Some pieces had a strong Southwestern motif, while others blended in elements of modernism. A visit with the family at the booth while viewing designs from four generations of jewelers illustrated the diversity of styles.

The Patania family has been making jewelry in the southwestern United States since 1927. Frank Patania Sr. was only nine years old when he emigrated from Sicily to the United States in 1909 following a devastating earthquake. He opened the Thunderbird Shop in Santa Fe, New Mexico, after leaving New York following a bout of tuberculosis. His son Frank Jr., grandson Sam, and great-grandson Marco have all followed in his footsteps, each with his own distinct style.

The Thunderbird Shop was initially a curio shop selling Navajo and Pueblo silver jewelry along with Native American blankets, rugs, pottery, baskets, beadwork, and paintings. Frank Sr. started selling his own silver and turquoise art nouveau and Native American-inspired pieces such as jewelry, boxes, belt buckles, spoons, and letter openers out of the shop in the 1930s (figure 31). With the help of his wife, Aurora Patania, and other family members, the Thunderbird Shop grew and became a popular Santa Fe destination for prominent artists such as Georgia O'Keeffe. In fact, a 1933 Alfred Stieglitz photograph shows her wearing one of the Thunderbird Shop's ridged silver bracelets, since renamed "Georgia" in her honor. Frank Sr. was known as a jewelry artist who brought a Mediterranean influence to silver and turquoise work. A second Thunderbird Shop was opened in Tucson in 1936.

As an apprentice to his father, Frank Jr., or "Pancho," carried forward the silversmithing tradition, expanding it to incorporate modern design concepts. He began entering



Figure 31. "Cleopatra" sterling silver necklace designed by Frank Patania Sr., featuring 99 Morenci turquoise stones. Photo by Robert Weldon; courtesy of Patania Jewelry.

pieces in juried shows and developed a reputation as a top U.S. designer in the contemporary art movement. Frank Jr. was known for his meticulous craftsmanship, not only in jewelry but also in liturgical items and abstract sculptures. Two of his cuff bracelets are in the permanent collection of the Smithsonian American Art Museum. Figure 32 shows a duplicate of one—the “Asymmetry” hollow-form bracelet, also known as the “Twin Peaks” bracelet.

Sam Patania studied under Frank Jr. for 10 years starting at age 14. After this training period, Sam began branching out with his own designs featuring metal texturing and shaping methods such as repoussé. He credits Danish silversmith Georg Jensen and American artist William Spratling as his inspirations. This year at AGTA, Sam’s ex-

pertise and passion for texturing was evident at his demonstration during the MJSA Journal LIVE session. Fig-



Figure 32. One of two identical silver hollow-form bracelets by Frank Patania Jr. This cuff, known as both “Asymmetry” and “Twin Peaks,” was made around 1960 from six pieces of sterling silver using a small superstructure for support during the soldering process. The cuff weighs 100 g and measures 7 cm (2.75 in.) at its widest point. Photo by Robert Weldon; courtesy of Patania Jewelry.



Figure 33. *Nebula series necklace* by Sam Patania, featuring sterling silver and spiderweb turquoise from the Number 8 mine in Nevada used for the pendant, while the necklace consists of turquoise beads from the Sleeping Beauty mine in Arizona. Photo by Sam Patania; courtesy of Patania Jewelry.

ure 33 shows an example of his work with turquoise and silver.

Sam's son Marco Patania is continuing the storied family tradition with silver forming, texturing, and stamping. Trained by his father for six years from the age of 13, with

additional training at the Haystack School of Craft in Maine, Marco draws inspiration from the mid-century modern vibe and the unique role of Los Alamos, New Mexico, in nuclear research during that era. He pays homage to these themes by incorporating vintage uranium-containing glass marbles into modern cuff designs (figure 34). These marbles fluoresce a bright yellowish green under ultraviolet light.

For nearly a century, the Patania family has followed a tradition of excellence in Southwestern and modern jewelry craftsmanship.

Jennifer Stone-Sundberg

The appeal of non-nacreous pearls. Pearls never disappoint at the AGTA and GJX shows, and this year was no exception. While quantities were lower, a good supply of Tahitian, freshwater, and South Sea pearls was available. AGTA hosted a booth sponsored by Martin Rappaport featuring nacreous natural pearls from Bahrain, complete with reports from DANAT, the Bahrain Institute for Pearls & Gemstones. Of particular interest was a wide selection of natural non-nacreous pearls.

Several vendors at GJX offered non-nacreous conch pearls, with a smaller selection available at the AGTA show. Alec Rupp-Smith of Aloha Pearls Hawaii showed a fabulous graduated, mixed-color conch pearl necklace (figure 35) at both the GJX and Pueblo shows. The necklace featured 37 conch pearls with a total weight of 179 carats. Thirty-two diamonds, 9.06 carats total, were used as accents to the suite of pearls.

Rupp-Smith also presented an interesting Melo pearl from Myanmar (figure 36). The pearl was clearly cut in half, with the other half likely fabricated into jewelry. The remaining 57 ct half was polished to display the fine concentric rings used to help separate bead-nucleated cultured pearls from their natural counterparts, without the need for X-ray tomography. The banding was visible even without a loupe.

Figure 34. *Silver cuff* by Marco Patania. Note the antique uranium glass marble beads that fluoresce under UV light (right) and the hand stamping on the interior. Photos by Robert Weldon; courtesy of Patania Jewelry.





Figure 35. Necklace featuring 37 conch pearls accented by 32 diamonds. Photo by Robert Weldon; courtesy of Aloha Pearls Hawaii.

Somewhere in the Rainbow returned to the AGTA show to highlight recent acquisitions to their ever-growing collection. The mission of the collection is to bring education and enjoyment of fine colored gems to museums, galleries, and facilities dedicated to preserving the rarity and beauty of these minerals, gems, and articles of jewelry. The collection features pearls and colored stones from a wide contingent of designers from around the world. This year,

three non-nacreous pearl creations stood out, sourced from Carlos Chanu, owner of California-based PCD Pearls.

The first was a *Cassis* pearl suite consisting of a graduated necklace and convertible ring/brooch all fabricated in 18K gold and platinum by designer Jim Grahil of Balboa Island, California (figure 37, left). Chanu sourced the pearls from Europe over the course of one year. The layout of the necklace took a month to get just right, with a nicely



Figure 36. Melo “half pearl” weighing 57 ct. Photo by Robert Weldon; courtesy of Aloha Pearls Hawaii.

matched blend of size, shape, and color. The ring/brooch pearl is one of the finest examples of *Cassis* known.

The second is the “Golash” brooch in figure 37 (right), named after the man who purchased it at an antique store

in 2000 for \$14, which dates back to 1835 and was fabricated in the state of Rhode Island. Two rare quahog pearls (*Mercenaria mercenaria*) are set in the piece. At 13.5 ct and 13 mm, the larger, slightly button-shaped pearl has a glass-

Figure 37. Left: Cassis pearl necklace and convertible ring/brooch designed by Jim Grahil. Right: “Golash” brooch featuring fine quahog pearls. Photos by Robert Weldon; courtesy of the Somewhere in the Rainbow collection.





Figure 38. Quahog (*Mercenaria mercenaria*) pearl suite offered at the GJX show. Photo by Robert Weldon; courtesy of Pacific Coast Pearls.

like surface and stunning color that make it an exceptional natural quahog pearl. *Mercenaria* pearls are rare, found as a byproduct of the clam fishing industry on the East Coast of the United States. The smaller, near-perfect drop-shape pearl measures nearly 9×7 mm and weighs 2.89 ct. Uniform natural drop pearls are among the rarest for any mollusk. As part of an international pearls exhibition, the "Golash" brooch toured the world from 2001 to 2008.

Pacific Coast Pearls (Henderson, Nevada) brought an impressive array of natural pearls to GJX this year. After owner Wes Rankin found his first abalone pearl while diving off the coast of California, he spent the next decade collecting and purchasing pearls. This led to what has become one of the largest selections of natural pearls on the market today. At the show, co-owner Tish Rankin assembled an extraordinary suite of quahog pearls, just waiting for the right designer and inspiration to come along (figure 38). If only the humble clam had known.

Eric Fritz

Thirty years later: "The Royal Tapestry" revisited. Three generations of the Piat family gathered at the University of Arizona Alfie Norville Gem & Mineral Museum in Tucson on February 1 to see "The Royal Tapestry" (see Spring 2022 GNI, pp. 110–111) for the first time. The tapestry (figure 39) was created by French master jewelry house Cristofol Paris more than thirty years ago, with Maison Piat (Paris) procuring the gemstones and facilitating their cutting. Prior to the gathering, Daniel Piat was the only family member who had seen the completed tapestry.

The tapestry contains almost 27,000 emeralds, diamonds, rubies, and blue and yellow sapphires as well as 37.5 lbs of 18K gold. Its 122×71 cm (42 × 24 in.) dimensions, the same as those of an Islamic prayer rug, were specified by the

royal family in the Middle East who privately commissioned it. More than 25 cutters matched the stone sizes within one-tenth of a millimeter. Cristofol Paris artisans spent more than 16,000 hours crafting the tapestry. Manufacturing a work of jewels that moved and flowed like a carpet or woven cloth required a form of prong setting, new at the time, that involved fewer "shared" prongs. Throughout the process, in a time before the advent of mobile phones and digital images, materials were shipped back and forth between Paris, Bangkok, Jaipur, and the Jura region of France.

Figure 39. Emmanuel and Daniel Piat (right) examine "The Royal Tapestry" together for the first time at the Alfie Norville Gem & Mineral Museum. Photo by Robert Weldon.





Figure 40. Left: Two Kashmir sapphire rough crystals: 77.00 ct unheated (left) and 25.20 ct heated (right). Right: Unheated Kashmir sapphires. Left to right: 1.29 ct pear shape, 2.60 ct cushion cut, 21.09 ct dragon carving, and 4.08 ct oval cut. Photos by Robert Weldon; courtesy of Eddie Cleveland of KashmirBlue and Jeffery Bergman of EighthDimensionGems.

The tapestry remained with the unnamed royal family until the early 2000s, when it was sold to a private collector. Prior to its exhibition in Tucson, it had been exhibited only in Hong Kong and London for one day each.

At the Alfie Norville Museum reception, board member Shelly Sergent touched on the origin of the tapestry concept and the process of transporting it from Zurich to Tucson. Daniel Piat shared the story of the tapestry's creation, describing the challenges presented by the design and the immense amount of work and detailed craftsmanship it required. Eric Piat noted the difficulty of sourcing the gems in a strict range of colors. Daniel said that after more than thirty years, all of the gems are still perfectly seated in more than 106,000 prongs and 26,649 seats, calling it "an engineering feat never duplicated in the jewelry world today."

Erin Hogarth
GIA, Carlsbad

New sapphire material from Kashmir. The legendary and remote sapphire mines of Kashmir, the disputed Himalayan territory between India and Pakistan, produced the finest-quality sapphires from 1890 through the 1920s. These coveted gems made their way south to Mumbai and eventually to Europe and America. Now, 100 years later, rough stones are still found, deposited through erosive processes. During the summer months, Kashmiri shepherds migrate north through the higher Himalayas, where they occasionally find sapphires in the riverbeds and on the hillsides. The glacier-tumbled rough typically exhibits rounded surfaces, affectionately referred to as "plums in pudding" by English geologist C.S. Middle in the 1930s (figure 40, left). Many in the trade believe the best available material dates back to five productive years in the 1880s.

Exhibited at the AGTA show by Jeffery Bergman (EighthDimensionGems, Bangkok) and Mayer & Watt (Maysville, Kentucky), this selection of newly found rough crystals, loose cut gems (figure 40, right), and mounted

Kashmir sapphires (figure 41) was all recently faceted by lapidary artisan Eddie Cleveland of KashmirBlue, who lived in Kashmir researching the historic mines for more than a decade. Cleveland uses his heat-treating experience to turn much of the pale grayish geuda-like rough to rich, well-saturated blues through standard high-temperature heating techniques. A limited amount of new material is found each year, and only a few pieces find their way to market.

Eric Fritz

Figure 41. Two untreated Kashmir sapphire rings. Top: 1.59 ct cushion-cut cornflower blue sapphire set in white gold with VVS baguette diamonds. Bottom: 1.00 ct oval-cut medium lighter blue sapphire set in an Art Deco style diamond platinum ring. Photo by Robert Weldon; courtesy of Eddie Cleveland of KashmirBlue and Jeffery Bergman of EighthDimensionGems.





Figure 42. Untreated Montana sapphire showing a variety of cuts and the range of in-demand green to blue hues available. The stones range in size from 3.34 ct (stone on the far right) to 5.78 ct (third from the left). Photo by Jennifer Stone-Sundberg; courtesy of Obsessed Over Gems.

Montana sapphire at Obsessed Over Gems. At the AGTA show, miner and owner Don Johnson (Obsessed Over Gems, Helena, Montana) showed us an array of unheated Montana sapphires in a range of hues, cuts, and sizes (figure 42) while describing what is in demand from his customers. Pale green is particularly popular, followed by pale blue.

“Silky” stones with a soft appearance were in high demand this year, an observation echoed by other vendors. The abundance of needle inclusions in some of Johnson’s silky stones rendered them translucent to virtually opaque, such as the dark green sapphire in figure 43 that he referred to as the “silk bomb.”

In response to the demand for natural colors and unaltered inclusions, Johnson has moved away from heat treating any newly mined sapphires. He has many of his stones pre-

cision cut by notable cutters, resulting in clean stones with so much fire that at first glance, one could mistake them for a stone with a much higher refractive index (figure 44).

For his larger and more significant stones, Johnson has been providing mine-to-market origin and traceability reports. These certifications document both the rough and the resulting cut stone. He uses two laboratory services (GIA and AGL) for each stone he deems important enough to provide this documentation for.

Johnson, along with many other vendors, sees no softening in the Montana sapphire market; in fact, it keeps getting stronger each year. He noted that the first day of the AGTA show this year was the busiest he has ever had. On that opening day, he sold almost all of the stones with origin and traceability reports that he had brought to Tucson.

Jennifer Stone-Sundberg

Figure 43. Three Montana sapphires showing a range of silkiness, from virtually none (2.80 ct green round cut by Craig Oliveira) to moderate (10.33 ct blue cushion cut by Victor Tuzlukov) to strong (21.20 ct hazy green “silk bomb” cut by Tuzlukov). Photo by Robert Weldon; courtesy of Obsessed Over Gems.



Figure 44. A 4.44 ct grayish violetish blue modified round brilliant Montana sapphire, precision cut by Joyce Wang to maximize light return. Photo by Robert Weldon; courtesy of Obsessed Over Gems.



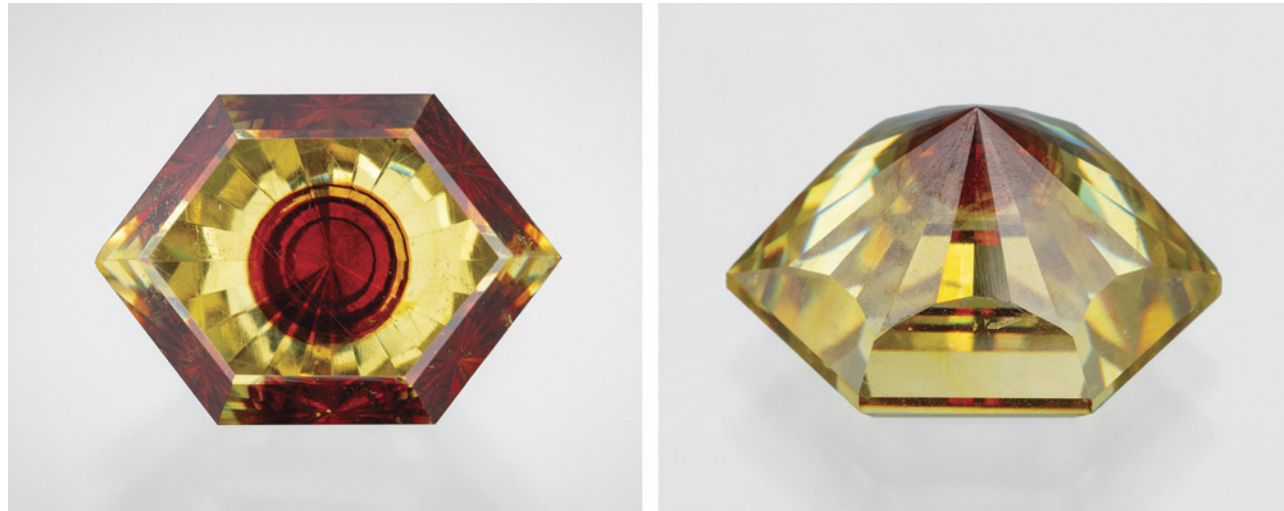


Figure 45. A 7.70 ct yellow sphalerite from Spain exhibiting a one-of-a-kind red circular center with distinct black rings. Face-up view of the pattern (left) and face-down view showing the careful placement of the red region by the cutter (right). Photos by Robert Weldon; courtesy of Dudley Blauwet Gems.

Unique sphalerite from Spain. Tucson is always full of surprises, and this year was no exception. At the AGTA show, Dudley Blauwet (Dudley Blauwet Gems, Louisville, Colorado) pulled a gem box out of his pocket to show the author a truly unique gem. This yellow sphalerite had a perfect red circle centered in the table with three sharp and distinct black rings encircling it (figure 45).

The stone was cut from material from Santander in Cantabria, Spain, a source known for producing the best facet-grade sphalerite in the world. The deposit yields orange and red stones that can be quite large, with some weighing hundreds of carats.

Sphalerite, a zinc sulfide (ZnS) mineral, is an important ore of zinc and rarely of gem quality. Colorless in its pure form, it goes from yellow to red to brown to a submetallic black color with the addition of iron. The presence of cobalt can cause a green color. Sphalerite has both an extremely high refractive index (2.37) and dispersion (>0.150), and when properly cut it can have significant brilliance. Despite these desirable gem qualities, sphalerite's softness (Mohs hardness of only 3.5 to 4.0), brittleness, and perfect cleavage make it a challenge to cut and polish (R.T. Liddicoat, *Handbook of Gem Identification*, Gemological Institute of America, Santa Monica, California, 1989).

This one-of-a-kind stone was expertly cut in Europe by an artisan who knew how to work soft, brittle stones with cleavage and how to properly center the red "dot" in the culet. The distribution of iron in this sphalerite crystal assumes distinct regions: sharply defined black rings with high iron saturation, a red circular area of medium saturation, and a surrounding area of lower saturation.

This exceptional sphalerite is proof that the combination of Mother Nature and a skilled cutter can reveal the infinite possibilities for spectacular gems.

Jennifer Stone-Sundberg

Out of Our Mines. As noted in the overview on pp. 90–93, turquoise was one of the most prolific gems in Tucson this year, found in a variety of jewelry, cut stones, and rough throughout the shows. Richard Shull and Helen Constantine-Shull of Out of Our Mines (Dyer, Nevada) reported strong sales at the AGTA show, where they had an impressive variety of mainly American stones, particularly turquoise and variscite from Nevada. They also offered other popular materials, including Oregon chalcedony, California tourmaline, Oregon sunstone, Nevada golden opal, and Arizona amethyst.

Childhood visits to trading posts during trips to the Southwest sparked Richard's fascination with turquoise and jewelry. His family's gold mining activities in California and Nevada inspired his own interest in mining. Helen similarly traveled throughout the Southwest as a child, developing a strong appreciation for the local rocks and plants. Both Shulls have extensive lapidary and jewelry-making experience. They began mining their own material in the late 1980s and became mine owners in the 1990s. Currently, they own and operate several turquoise and variscite claims in Nevada.

Helen attributed her passion for turquoise and variscite to their great variety of patterns and colors. Their highest-end turquoise is material with tight, distinct spiderweb patterning from their Black Widow and Black Web Gem mines. Only about two pounds of material has been recovered to date from the Black Web Gem mine, and it is some of the finest natural black web turquoise in the world (figure 46). Also popular are greens from the Northern Lights mine, bright greenish blue material with striking reddish brown matrix from the Double Eagle mine, blues with strongly contrasting matrix from the Nevada Blue mine, and pattern-free clear gem material from the Supernova and Aztec mines at Royston (figure 47).



Figure 46. Extremely rare Black Web Gem mine turquoise nuggets and cabochons from Nevada. These pieces are natural with no treatments except for the backings added to the cabochons. The center oval is approximately 16 × 12 mm. Photo by Richard Shull; courtesy of Out of Our Mines.

Turquoise with distinct matrix patterning is a strong draw for those seeking one-of-a-kind pieces, a very popular trend in jewelry today. However, there is still solid demand for clear gem material, which the Shulls sell from both vintage sources (1950s Persian) and from their own Dyer Blue and Supernova mines in Nevada, which both produce webbed and clear turquoise (figure 48).

Variscite, a non-copper-containing aluminum phosphate mineral closely related to turquoise, is gaining popularity as consumers learn more about this mineral. Variscite comes in a range of greens and can exhibit the same fascinating matrix patterns found in turquoise (figure 49).



Figure 47. Natural Nevada turquoise from the Nevada Blue mine (stone farthest to the right, the pear shape on top, and the large center triangle); the Double Eagle mine (freeform triangular stone on center right and the geometric freeform below that); the Northern Lights mine (green stone); the Black Widow mine (two tight spiderweb stones on the left); and calibrated stones from the Supernova and Aztec mines at Royston (clear gem material without patterning). Sizes range from 2.12 ct to 24.62 ct. Photo by Robert Weldon; courtesy of Out of Our Mines.

The Shulls described how some buyers form a personal connection with the material. For these customers, the stone they acquire is more than simply a piece of turquoise; it is a stone from a known location, uncovered by a known person, with a clear story of how it reached the final form in front of them.

Jennifer Stone-Sundberg



Figure 48. Stabilized Nevada turquoise from the Supernova mine. Sizes range from 5.61 to 13.09 ct. Photo by Robert Weldon; courtesy of Out of Our Mines.



Figure 49. Variscite with matrix (left) and clear gem variscite without patterning (right). Photos by Jennifer Stone-Sundberg; courtesy of Out of Our Mines.

Ukrainian pegmatitic heliodor and topaz. This year in Tucson, exceptionally large, clean, and attractively colored topaz and beryl from the Volodarsk-Volynskii pegmatite field in Ukraine (also known as the Volyn deposit) were very popular at multiple shows.

The Volyn deposit is in the northwestern portion of Ukraine, about 190 km from Kyiv. This deposit has been worked for more than 100 years and was initially mined for piezoelectric quartz with topaz as a byproduct. More recently it has been known for producing large and fine-quality topaz and beryl crystals as well as phenakite (Be_2SiO_4) and fluorite. The topaz ranges in color from blue to a golden-red sherry color, while the beryl ranges from mainly yellow heliodor to green beryl to greenish blue aquamarine. The large, beautifully etched heliodor crystals brought international notice to this deposit in the 1980s (G. Franz et al., "Etch pits in heliodor and green beryl from the Volyn pegmatites, northwest Ukraine: A diagnostic feature," Fall 2023 *G&G*, pp. 324–339).

At the GJX and Pueblo shows, Nomad's (New York City) had high-quality heliodor and topaz that were carefully cut to retain the beautiful rough etching patterns characteristic of this material (figure 50, left). These intricate etching patterns were retained in each gem's pavilion and visible face-up through the polished table (figure 50, right). The founders and owners are from Ukraine, and they started Nomad's in the 1990s with pegmatite minerals from Volyn.

At the AGTA and Pueblo shows, Dudley Blauwet Gems (Louisville, Colorado) featured topaz, heliodor, and phenakite from Volyn, which they have successfully been carrying for three years. This year, however, the demand for these Ukrainian gems has grown. In fact, Ukrainian topaz was one of their best sellers, with much of the material gone by the first day of AGTA. The bicolor blue to sherry topaz was a particularly strong seller, followed by blue topaz (figure 51). They noted that the miner they work with has been reworking old pockets for the last 20 years, and all of the topaz stones they offered in Tucson this year

Figure 50. Left: This 109.68 ct heliodor and 80.62 ct bicolor topaz are from the Volyn deposit in Ukraine. They are cut to leave natural etch faces on the pavilion/culet, while the crown and table are faceted. Right: A 162.22 ct pear-cut heliodor. The natural etching patterns are retained on the pavilion and are well displayed through the polished table. Photos by Robert Weldon; courtesy of Nomad's.





Figure 51. Exceptionally large and clean blue and bi-color topaz from the Volyn deposit. The blue triangular cut is 113.86 ct, the middle blue cube cut is 87.82 ct, and the blue and golden bicolor rectangular cut is 55.70 ct. Photo by Robert Weldon; courtesy of Dudley Blauwet Gems.

were from the same pocket at a depth of about 35 meters in the central part of the Volyn deposit.

The beauty, size, and availability of the gem crystals from these pegmatites bodes well for the continued presence of this material in the marketplace.

Jennifer Stone-Sundberg

*Wim Verriest
GIA, Bangkok*

Gold granulation by Zaffiro. Granulation, an ancient goldsmithing technique dating back nearly five millennia to Mesopotamia, involves the joining of tiny high-karat gold or other precious metal spheres ("granules") to a metal

base to create a decorative pattern (J. Wolters, "The ancient craft of granulation," *Gold Bulletin*, Vol. 14, No. 3, 1981, pp. 119–129). These patterns can be very complex, and the granulation process is one that requires a high level of precision.

In the AGTA designer showroom, we spoke with Jack and Elizabeth Gualtieri of Zaffiro (Walla Walla, Washington; figure 52), who specialize in 22K gold granulation. They occasionally incorporate platinum as well. They find the granulation technique very rewarding and meditative, as it demands extraordinary focus.

The Gualtieris formed Zaffiro in 1996 in Portland, Oregon, after meeting at the University of Kansas several years earlier. Their focus on granulation was inspired by a seminar at the university and by Elizabeth's study abroad in Florence. They chose the name "Zaffiro," which translates to sapphire in Italian. The business was a part-time venture until they could dedicate themselves to it full-time starting in 2003. They have sold their pieces through galleries, retail shows, and private clients. In 2019, they moved to Walla Walla.

Figure 52. Elizabeth and Jack Gualtieri of Zaffiro at their AGTA booth. Photo by Jennifer Stone-Sundberg.





Figure 53. “Where the Ocean Meets the Sky” is a one-of-a-kind pendant featuring a 19.51 ct Australian boulder opal and 11.37 carats of blue moonstone. The boulder opal is accented with 0.63 carats of tsavorite garnet. The granulated yellow gold is 22K, and the gold links between the elements are 18K yellow gold. Photo by Robert Welldon; courtesy of Zaffiro.

Jack and Elizabeth design and construct each piece from start to finish and consult with each other on their individual designs. They alloy their own 22K yellow, white, and rose gold and also create their own gold sheet, wire, and granulation balls. After clipping snippets of wire onto charcoal blocks, the blocks are heated to bead the metal into tiny

balls of gold, which are then sorted by size through sieving. (To watch a video showing the process of fabricating granulation balls, please go to www.gia.edu/gems-gemology/spring-2024-gemnews-gold-granulation).

The Gualtieris find inspiration in the stones they purchase, the natural world around them, and architecture. In



Figure 54. Tanzanite pendant designed and fabricated by Elizabeth Gualtieri containing a 46.15 ct tanzanite crystal in a hand-fabricated setting of granulated 22K gold. Photo by Robert Weldon; courtesy of Zaffiro Jewelry.

fact, they sometimes have to negotiate over who will get to use a particular stone, as both artists may simultaneously envision designs for it.

Jack's opal, moonstone, and tsavorite garnet pendant design (figure 53) began with the Australian boulder opal. The moonstones inspired him to go larger with the design

and add some movement to the piece. He said the use of green tsavorite garnet accent stones around the opal instead of blue stones was a riskier option but ultimately the right choice.

A heated rough tanzanite crystal inspired the pendant designed and built by Elizabeth in figure 54. This piece rep-



Figure 55. Suhuan Wang's winning necklace design sketch for the 2023 Gianmaria Buccellati Foundation Award for Excellence in Jewelry Design, featuring platinum, emerald, ruby, diamond, and tsavorite.

resents a signature style the Gualtieris describe as "talismans," signifying the way in which collectors of the pieces connect with them. This jewelry collection features rough crystals or baroque pearls and represents some of Zaffiro's most personal pieces. The intricate caps allow for a more expressive use of granulation and accent stones.

The fusion of this ancient technique with contemporary jewelry designs is a testament to the timelessness of granulation and its endless design possibilities.

Jennifer Stone-Sundberg

ANNOUNCEMENTS

Seventh annual Gianmaria Buccellati Foundation Award winner. Suhan Wang, a graduate of GIA's Jewelry Design program in Taiwan, received the seventh annual Gianmaria Buccellati Foundation Award for Excellence in Jewelry Design. The 18 finalists and winner were announced at the GIA Alumni Collective's "Night at the Museum" event held during the AGTA GemFair in Tucson. Wang's winning design, a necklace featuring platinum coils

adorned with emerald, ruby, diamond, and tsavorite, stood out to the judges for its sense of movement and skill of execution (figure 55).

Created in partnership with the Gianmaria Buccellati Foundation in 2018, the award recognizes outstanding talent in design among GIA students worldwide. Larry French, chief officer for North American strategies at the foundation, said, "On behalf of the Gianmaria Buccellati Foundation and Rosa Maria Buccellati, we want to congratulate Ms. Suhan Wang, plus all the other designers whose work has honored this competition. We also want to send our appreciation to the talented GIA design instructors whose skill and efforts helped the students on their journey to celebrate the art of jewelry design in the highest way, an art that meant so much to Gianmaria Buccellati."

As part of the award, Wang will travel to Italy and meet with a representative from the foundation.

The 2024 Gianmaria Buccellati Foundation Award for Excellence in Jewelry Design competition is underway and open to students in GIA's Jewelry Design courses who meet the eligibility requirements. Visit www.gia.edu/buccellati-foundation-award-jewelry-design for more information.

Take the 2024

GEMS &
GEMOLOGY

CHALLENGE

Test your gemological knowledge! Scan the QR code to take the GEMS & GEMOLOGY Challenge quiz online (see pp. 56–57 of this issue). Answers must be submitted by September 1, 2024.



REGULAR FEATURES

COLORED STONES AND ORGANIC MATERIALS

Unusual aquamarine–white beryl. Recently, the author analyzed an interesting 41.51 ct faceted bicolor beryl (figure 1) composed of aquamarine and opaque white beryl. This gem belongs to Brazilian gem dealer Veber Leite and is part of his collection containing several similar specimens. According to Leite, the bicolor beryls were mined in Brumado, a city located in the state of Bahia, Brazil, but their geographic origin could not be confirmed.

Standard gemological testing of both sections revealed a specific gravity of 2.70 and a refractive index of 1.581–1.592. Ultraviolet/visible/near-infrared (UV-Vis-NIR) spectra revealed an absorption band centered at about 810 nm, also present in both sections. In beryl, this band is associated with Fe²⁺ (D.L. Wood and K. Nassau, "The characterization of beryl and emerald by visible and infrared absorption spectroscopy," *American Mineralogist*, Vol. 53, No. 5, 1968, pp. 777–800; Y. Hu and R. Lu, "Color characteristics of blue to yellow beryl from multiple origins," Spring 2020 *G&G*, pp. 54–65) and possibly enhanced by neighboring Fe³⁺ (S. Sae-seaw et al., "Geographic origin determination of emerald," Winter 2019 *G&G*, pp. 614–646). The blue section exhibited an anisotropic band around 600 nm when viewing an e-ray oriented absorption spectrum, typical of aquamarine (Hu and Lu, 2020). The white color was caused by an isotropic absorption band ranging from 400 to 700 nm with a nearly identical absorption coefficient through all wavelengths.

Although seemingly opaque, when exposed to the polariscope's intense light source, the white portion allowed the

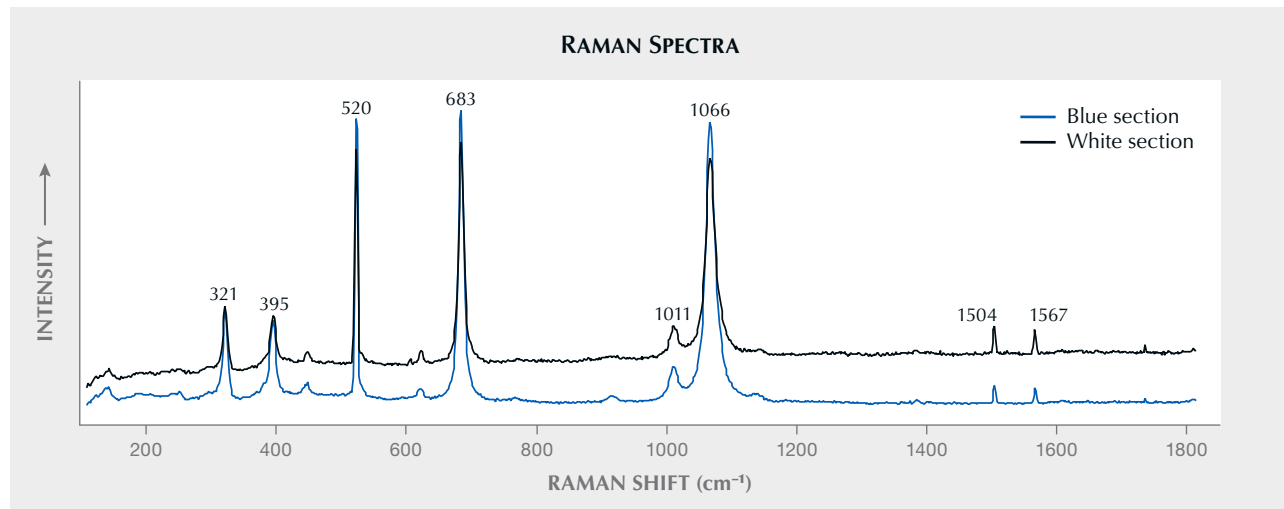


Figure 1. A 41.51 ct freeform faceted bicolor beryl.
Photo by Marina Boncompagni.

passage of light and showed no extinction under crossed polarizers, suggesting a polycrystalline composition.

Raman spectra were collected at room temperature using a Horiba Scientific LabRAM HR Evolution spectrometer coupled with an Olympus Scientific Solutions BX-41 microscope with a 50× magnification lens. The acquisition time was 120 seconds, grating: 500 nm. For this analysis, a 532 nm excitation laser was selected. Both sections exhibited major peaks around 321, 395, 520, 683, 1011, and 1066 cm⁻¹ (figure 2). Minor peaks were observed at 448, 622, and 1141 cm⁻¹. The spectra were compatible with beryl and, although clarity treatment was not observed, displayed relatively strong absorptions at approximately 1504 and 1567 cm⁻¹ (again, see figure 2) that may suggest the presence of a filling agent (M.L. Johnson et al., "On the identification of various emerald filling substances," Summer 1999

Figure 2. The Raman spectra of the blue and white sections in the 41.51 ct bicolor beryl. Spectra are offset vertically for clarity.



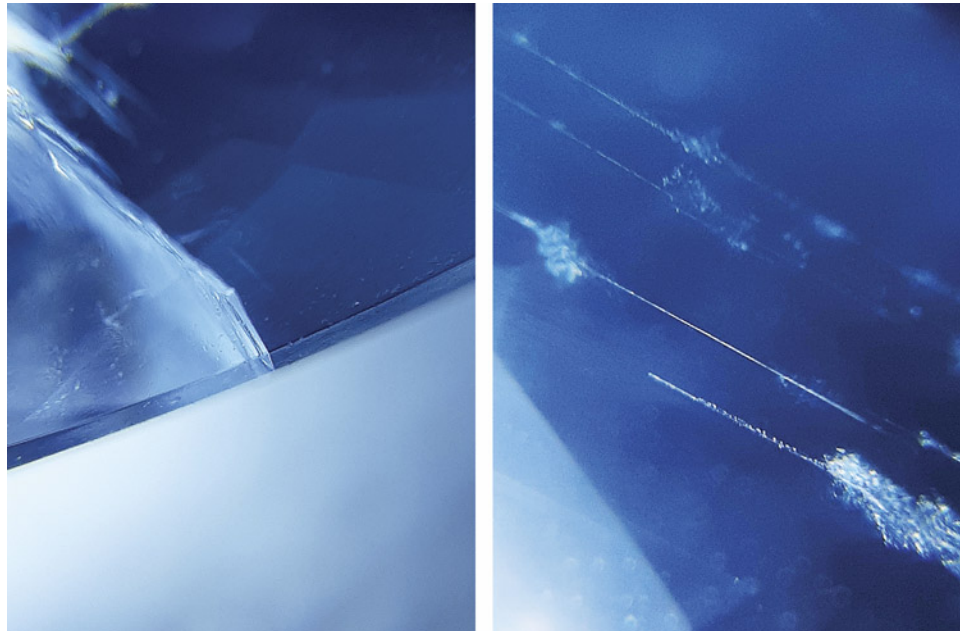


Figure 3. Left: The aquamarine–white beryl boundary. Right: Beryl channels parallel to aquamarine’s c-axis in the blue portion of the bicolor beryl.
Photomicrographs by Marina Boncompagne; field of view 10.00 mm.

Ge&G, pp. 82–107). Additional Raman analysis with a spectral range of 100–3500 cm⁻¹ is required to determine whether the peaks are indeed related to a filling substance.

Microscopic analysis revealed a well-defined aquamarine–white beryl boundary (figure 3, left). Channels parallel to the *c*-axis were also observed (figure 3, right).

The author is aware of similar aquamarine–white bicolor beryl from the state of Minas Gerais, but this was the author’s first encounter with such beryl reportedly from Brumado, Bahia.

Acknowledgments: The author thanks Professor Ariete Righi from the physics department of the Federal University of Minas Gerais (DF-UFMG) for providing the Raman analysis.

Marina Boncompagne
Federal University of Espírito Santo (UFES), Brazil

Beryl from Newfoundland, Canada. Prospectors Art Gardner and Terry Russell recently discovered concentrically zoned beryl [Be₃Al₂[Si₆O₁₈]] in central Newfoundland, Canada, along the Bay D’Espoir Highway, and sent preliminary findings to GIA’s Carlsbad laboratory. The green rims of these beryls were often sufficiently green to be considered emerald. The outer rims were bright green or pale green, and the cores were very pale green or white (figures 4 and 5). Most zones had low transparency. They formed hexagonal columns at the 1–3 cm scale, associated with mica-quartz-feldspar veins and minor tourmaline, calcite, biotite, fluorite, pyrite, and arsenopyrite. Some stones were suitable for polishing and setting in jewelry, especially as cabochons. An individual specimen may have zones that fit into the definitions of emerald and white beryl, with the brighter greens at the rims.

Canada is host to a number of gem minerals, including emerald from Yukon and the Northwest Territories (G.



Figure 4. Emerald and beryl specimens from Newfoundland, Canada. The chip on the right has a distinct green rim in this position, on its lower right edge.
Photo by Emily Lane; courtesy of Art Gardner and Terry Russell.



Figure 5. In situ emerald and beryl from Newfoundland. The primary crystal shows a lively green hue. The crystal on the lower right shows strong concentric zonation with a green rim and a white core. Photo by Emma Hutchinson Photography; courtesy of Art Gardner.

Giuliani et al., “Emerald deposits: A review and enhanced classification,” *Minerals*, Vol. 9, 2019). This beryl deposit on Newfoundland Island is within the Great Bend Complex of ophiolites. The mica-quartz-feldspar veins hosting the beryl are found within a host rock rich with scheelite [Ca(WO₄)]. Other pegmatitic dikes are regularly found within the bedrock, and a ~450 km belt of beryl-bearing pegmatite dikes extends across the island from east to west. This discovery adds another locality to Canada’s gemological map.

The ultraviolet/visible/near-infrared (UV-Vis-NIR) absorption spectrum of the green zone in the leftmost crystal in figure 4 displayed absorption bands at 420 (Fe³⁺), 615 (V³⁺,

Cr³⁺), and 835 nm (Fe²⁺) and a sharp but low absorption peak at 956 nm (H₂O) (figure 6). These are due to the combined effects of vanadium and iron, with minor influence of chromium. These features are common in emerald.

The beryls’ chemistry, as determined by laser ablation-inductively coupled plasma-mass spectrometry (LA-ICP-MS), is unique from other worldwide deposits; both the white cores and green rims had elevated lithium and cesium (figure 7). The lithium and cesium values are within the range expected more of a beryl from a lithium-cesium rich pegmatite, such as many morganites or goshenites. The green coloration is primarily due to vana-

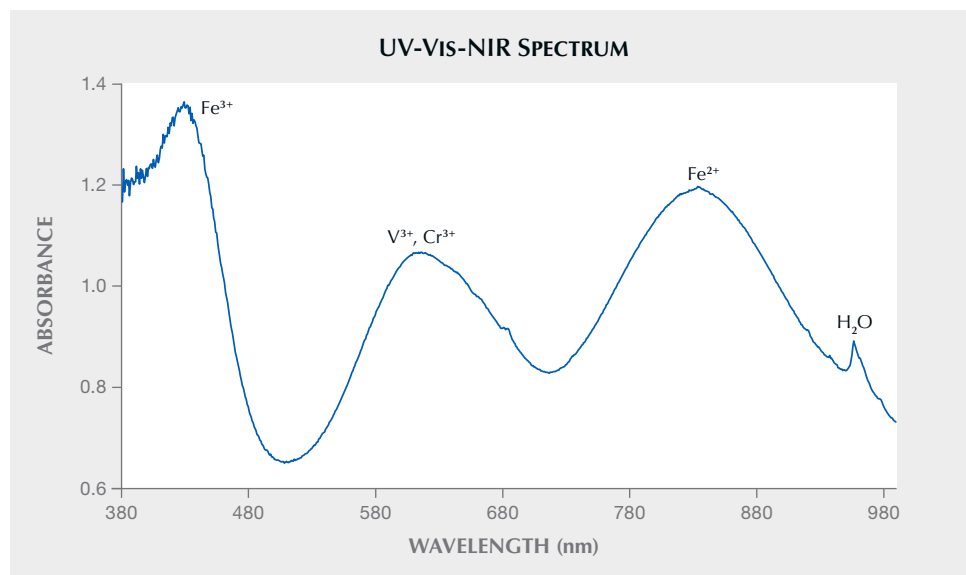


Figure 6. UV-Vis-NIR absorption spectrum of the first crystal on the left in figure 4. Absorption bands are seen at 420, 615, and 835 nm, and a low but sharp peak at 956 nm.

TABLE 1. Composition ranges (in ppm) for significant minor elements in Newfoundland emeralds, measured by LA-ICP-MS.

Sample area	Li	Na	Mg	V	Cr	Fe	Cs
Green rims	1100–1310	9980–11200	5290–8210	1000–2100	11.8–213	1500–2330	4260–5180
White cores	2000–2290	8070–9640	1630–3570	52.7–270	0.93–7.77	723–903	2630–3240
Detection limit (ppm)	0.06	2	0.05	0.01	0.3	2	0.02

dium, with minor chromium, which are both chromophores of emerald (table 1). The magnesium is consistently higher than iron, as expected for emeralds (R.E. Henry et al., “Crystal-chemical observations and the relation between sodium and H₂O in different beryl varieties,” *Canadian Mineralogist*, Vol. 60, 2022, pp. 625–675). The magnesium and transition metals are higher in the green rims than in the white cores, which have higher lithium. However, the cesium is higher in the green rims. This is likely due to the near-mutual exclusivity of beryllium site and aluminum site cation substitutions, preventing significant lithium substitutions when there is a high level of magnesium and transition metals (R.E. Henry et al., “Predicting the crystal structure of beryl from the chemical composition,” *Canadian Journal of Mineralogy and Petrology*, Vol. 61, No. 4, 2023, pp. 873–897). As magnesium and iron require charge balancing, sodium and cesium can

serve this purpose; while cesium is associated with lithium in geologic environments, it does not have the same crystal-chemical constraints as lithium in beryl.

These beryls’ formation at the intersection of an ophiolite and a pegmatite is consistent with conditions required to create emerald as it brings together a source of vanadium or chromium with a source of beryllium. The goshenite cores are a feature that have been seen in emeralds from some other localities, including Russian emeralds.

Due to their uniquely high cesium and lithium, emerald zones of beryl from this locality are easy to differentiate. Should gem-quality specimens come to the market, a method is in place to confirm their origin as Newfoundland. Efforts are underway to continue exploration for additional gem material.

Rhiana Elizabeth Henry
GIA, Carlsbad

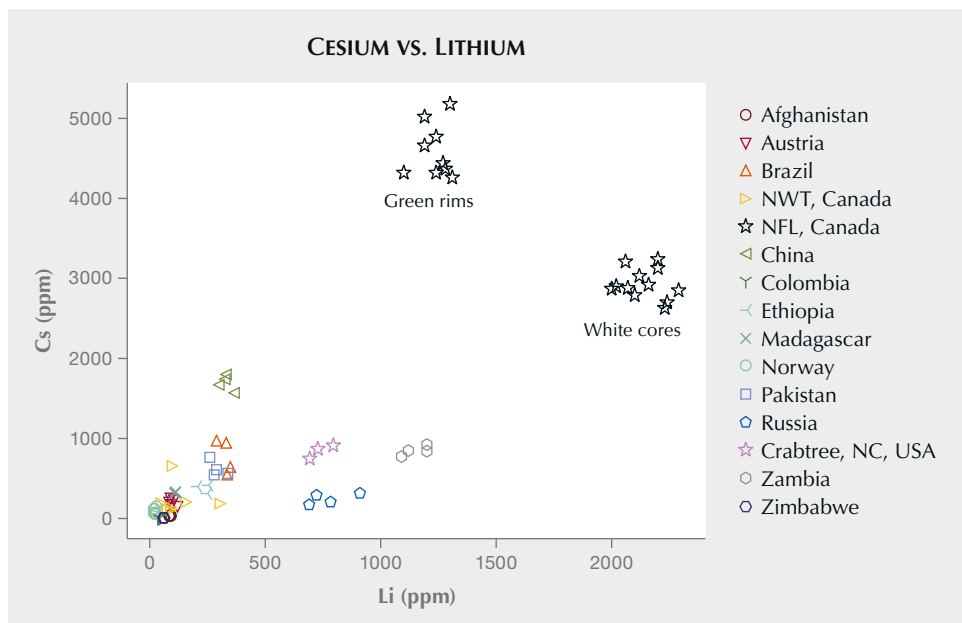


Figure 7. Cesium vs. lithium for emerald from worldwide localities, demonstrating the unique chemistry of Newfoundland (NFL) emeralds. Worldwide emerald data from GIA laboratories.



Figure 8. Cat's-eye emerald (11.31 ct) and star emerald (4.99 ct) from Chitral, Pakistan. Photo by Lhapsin Nillapat; courtesy of Mohammed Ayub (Pretty Little Gem Co., Ltd, Bangkok).

Phenomenal emeralds from Chitral, Pakistan. In November 2023, GIA researchers had the chance to study a parcel of emeralds reportedly from Chitral in Pakistan. All of the stones matched previously documented characteristics of emeralds from Chitral (C.S. Hanser et al., “Comparison of emeralds from the Chitral District, Pakistan, with other Pakistani and Afghan emeralds,” *Journal of Gemmology*, Vol. 38, No. 6, 2023, pp. 582–599).

Among the stones were two cabochons that showed unusual phenomena: chatoyancy and asterism (figure 8). Both had a refractive index of 1.57 (spot reading) and a yellowish green to green color, which identified them as emerald.

Cat's-eye emeralds are found in a number of locations, most notably Brazil and Colombia. The effect is caused by large concentrations of fine parallel tubes. Proper orientation of these linear features during cutting can result in a sharp, centered cat's-eye when the tubes reflect light.

Star emeralds are even rarer, with most originating from Brazil and Madagascar. The effect is usually caused by very small thin films that reflect light. The proper orientation of the cabochon dome with respect to tiny platelets can result in a six-rayed star that moves across the curved surface of the stone. In this emerald, some of the platelets that create the lower left arm are highlighted by iridescent reflective colors.



Figure 9. A 1.59 ct red musgravite. Photo by Shunsuke Nagai.

To our knowledge, these are the first phenomenal emeralds from Chitral, and they offer prime examples of lesser-known phenomenal emeralds.

*Wim Verriest
GIA, Bangkok*

Identification of chromium-bearing red gemstones using photoluminescence: A red musgravite case study. Photoluminescence (PL) provides us with useful information to understand physical properties of gem materials and can also be used for gem identification and treatment detection. For example, a 1.59 ct red musgravite (figure 9) that had previously been examined by the Central Gem Laboratory in Japan (Z. Zhenghao et al., “A remarkable Cr-bearing red musgravite,” *Journal of Gemmology*, Vol. 38, No. 6, 2023, pp. 548–551) was also submitted to GIA’s Tokyo laboratory for identification. Its standard gemological properties (refractive index, specific gravity, dichroism, and UV fluorescence reaction), Raman spectrum, and ultraviolet/visible spectrum were consistent with musgravite. The chemical formula was measured as $\text{Be}_{1.21}(\text{Mg}_{1.95}, \text{Fe}_{0.01}, \text{Zn}_{0.02})\text{Al}_{5.86}\text{O}_{12}$ by laser ablation-inductively coupled plasma-mass spectrometry (LA-ICP-MS) with a chromium concentration of 1360–1840 ppm (table 1). A PL spectrum for musgravite (figure 10) was also collected with a 532 nm laser and consisted of two strong

TABLE 1. Trace-element concentrations (in ppmw) of the red musgravite sample, measured by LA-ICP-MS.

	Ti	V	Fe	Cr	Zn
Concentration	50.4–160	120–275	366–473	1360–1840	2440–2800
Detection limit (ppmw)	0.7	0.07	5	0.6	0.2

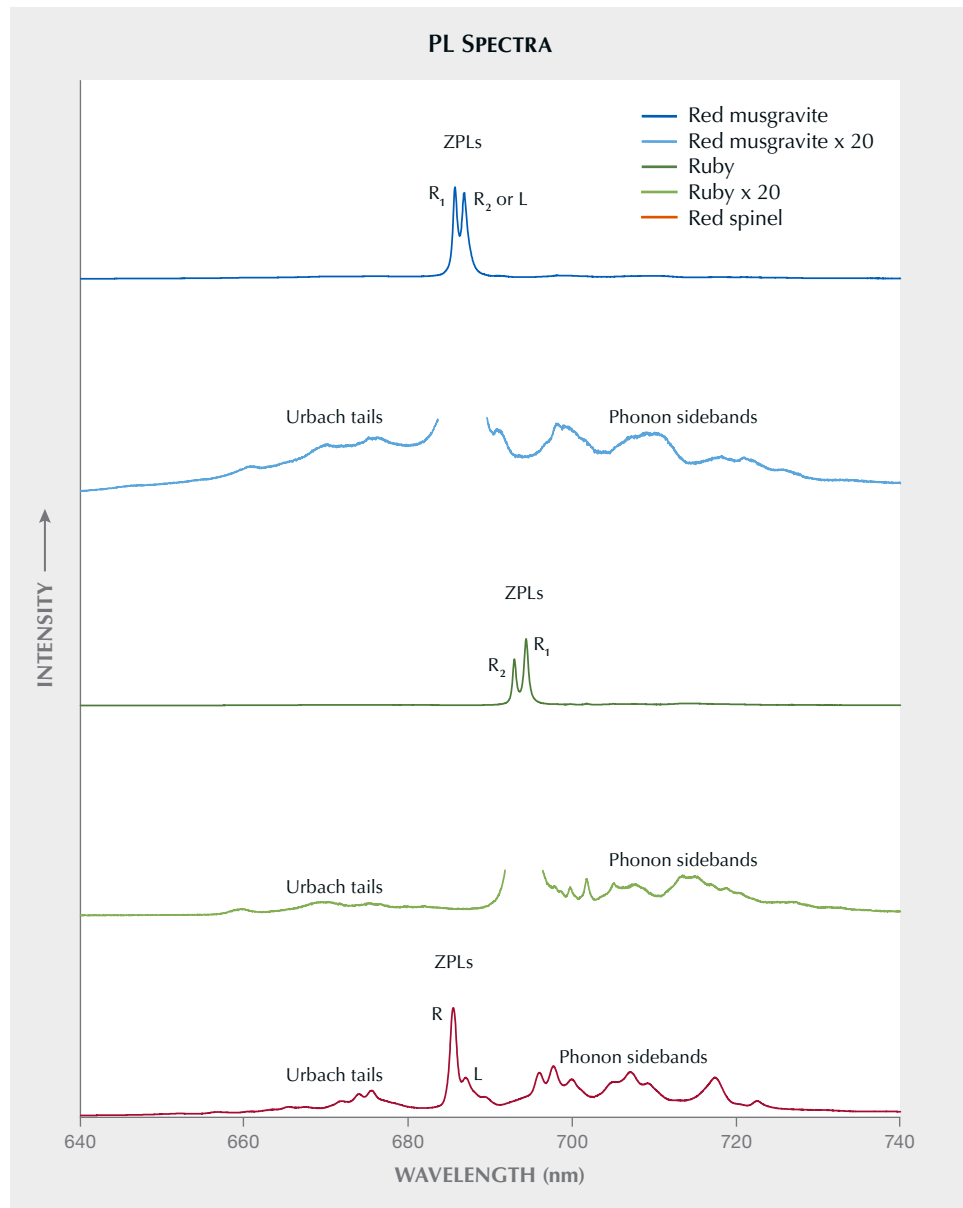


Figure 10. The PL spectrum of the red musgravite consisted of two very strong peaks at 685.7 nm (R_1) and 686.8 nm (R_2 or L). In the spectrum below that, its weak side peaks are expanded by multiplying the intensity by 20. They are partially similar to those of ruby (692.9 (R_2) and 694.4 (R_1) nm), its expanded weak side bands, and a red spinel (685.5 (R) and 687.1 (L) nm). Spectra are offset vertically for clarity.

peaks and weak side bands. Interestingly, the positions of the strong peaks were close to those caused by chromium in spinel, but the overall pattern was similar to that caused by chromium in ruby or sapphire. PL emission spectra are collected by exposing a material to strong short wavelength light, creating excited energy states in the material. These excited energy states then relax and return to a ground state by emitting light at a longer wavelength than the excitation wavelengths. The light collected during this relaxation is the PL spectrum. Trace amounts of chromium in many materials can easily enter these excited energy states and produce characteristic PL spectra in different gems such as ruby, spinel, and musgravite.

In this report, we investigated the reasons why these PL spectra differ between red musgravite, ruby, and spinel. The

two strong peaks at 685.7 and 686.8 nm of the red musgravite are referred to as zero-phonon lines (ZPLs) that do not contain the energy of “lattice vibrations,” which are the motions of atoms around their equilibrium positions. These peaks result from the transition from the lowest excited state to the ground state of three 3d orbital electrons of the Cr^{3+} ion replacing the Al^{3+} ion at the center of oxygen polyhedra, as in ruby and red spinel. The crystal structure of musgravite includes one type of AlO_4 tetrahedron and three types of AlO_6 octahedron: one undistorted and two differently distorted; see figure 11A, drawn using VESTA software (K. Momma and F. Izumi, “VESTA 3 for three-dimensional visualization of crystal, volumetric and morphology data,” *Journal of Applied Crystallography*, Vol. 44, 2011, pp. 1272–1276) and the reported crystal structure

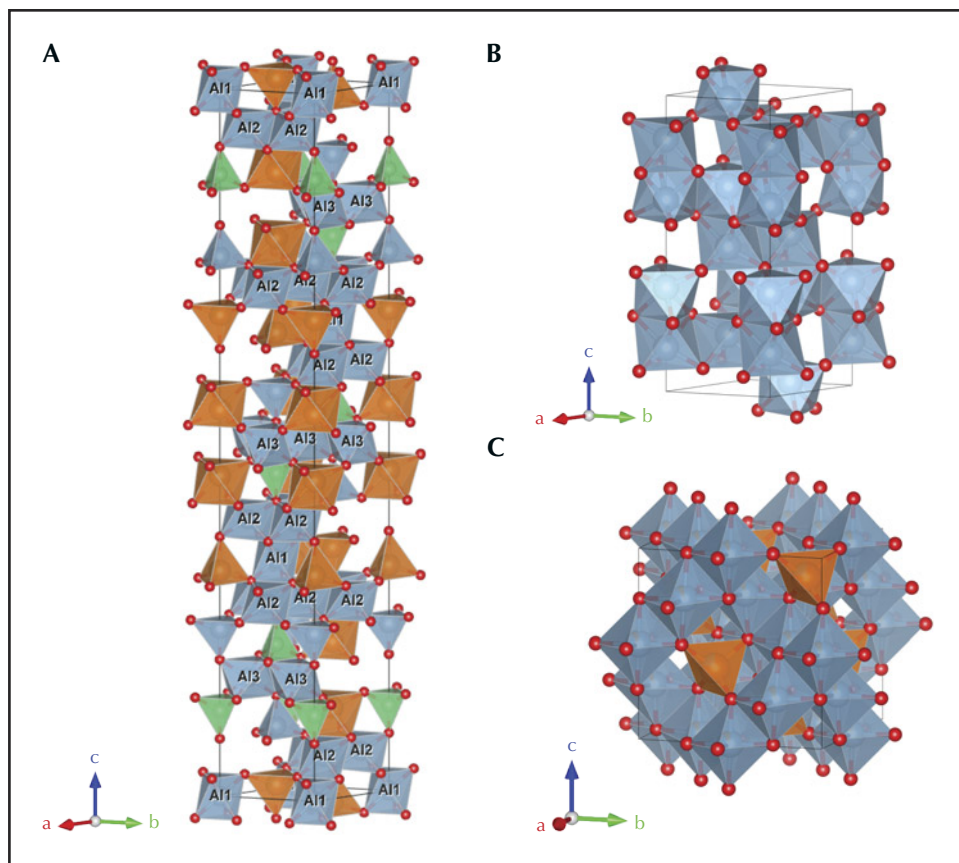


Figure 11. Polyhedral representations of the crystal structures of (A) reported musgravite, $\text{BeMg}_{1.63}\text{Fe}_{0.37}\text{Al}_6\text{O}_{12}$ (Nuber and Schmetzter, 1983); (B) typical corundum, Al_2O_3 ; and (C) normal spinel, MgAl_2O_4 . Thin black lines depict the unit cells. The green tetrahedra are BeO_4 . The orange tetrahedra and octahedra are MgO_4 and MgO_6 , respectively. The blue tetrahedra and octahedra are AlO_4 and AlO_6 , respectively. In musgravite, the AlO_6 octahedra have three types: one undistorted (Al1) and two differently distorted (Al2 and Al3).

data (B. Nuber and K. Schmetzter, “Crystal structure of ternary Be-Mg-Al oxides: taaffeite, $\text{BeMg}_3\text{Al}_8\text{O}_{16}$, and musgravite, $\text{BeMg}_2\text{Al}_6\text{O}_{12}$,” *Neues Jahrbuch für Mineralogie, Monatshefte*, 1983, pp. 393–402). The chromium PL emission is split into two strong lines, due to either the distortion of the AlO_6 octahedron as in ruby and sapphire, or the occupation of multiple crystal sites by chromium. The position of the red musgravite is shorter in wavelength than in ruby and sapphire but almost equal to that of red spinel. This means the energy difference between the excited and ground states is greater than that in ruby and close to that in red spinel.

The chromium PL spectrum for musgravite shows additional small peaks at longer and shorter wavelengths, termed “phonon sidebands” and “Urbach tails,” respectively (again, see figure 10). If the intensity of the main ZPLs is a large proportion of the total luminescence intensity, it indicates that the Debye-Waller factor, representing the magnitude of atomic vibrations in a crystal structure, is small. The weak sidebands on both sides of the red musgravite indicate that the Debye-Waller factor is smaller than that of red spinel but similar to ruby.

PL spectroscopy on chromium-bearing gemstones is not only one of the most powerful tools for quick and non-destructive identification but also a means to obtain interesting physical properties of rare gemstones by comparing

with the PL spectra of familiar gems. Furthermore, the difference in degree of the Debye-Waller factor may be one of the reasons why the presence or absence of heat treatment can be detected by PL in spinel (S. Saeseaw et al., “Distinguishing heated spinels from unheated natural spinels and from synthetic spinels: A short review of on-going research,” <https://www.gia.edu/doc/distinguishing-heated-spinels-from-unheated-natural-spinels.pdf>, April 2, 2009), but not in corundum.

Taku Okada and Makoto Miura
GIA, Tokyo

Challenges in identifying drilled keshi pearls. Distinguishing natural pearls from non-bead cultured (NBC) pearls, commonly referred to as “keshi” in the industry, has become increasingly complex. While traditional methods such as radiomicrography were once reliable for the identification of South Sea keshi NBC pearls, recent advances in pearl drilling techniques have rendered these conventional approaches less foolproof. As a result, there is a growing need for advanced data analysis to study the internal structure, chemistry, and other spectral features associated with the mollusk origin to enable reliable separation of natural from NBC pearls.

To further examine challenging structures, GIA’s Mumbai laboratory borrowed pearls represented as natural from

a known source. The lot consisted of 40 white to light cream drop and oval pearls (28 undrilled, 7 drilled, and 5 partially drilled). The smallest weighed 0.62 ct and measured 5.17×4.16 mm, and the largest weighed 2.95 ct and measured 9.53×6.65 mm (figure 12). The pearls all looked new, with smooth, high-luster surfaces that were free of blemishes. Under 40 \times magnification, the surfaces showed well-defined overlapping fine aragonite platy structures that accounted for their silky surface sheen.

Energy-dispersive X-ray fluorescence revealed manganese levels ranging from below detection level to 33.80 ppm and higher strontium levels ranging from 1756 ppm to 3364 ppm. Most of the pearls showed an inert reaction under X-ray fluorescence, while some had a weak yellowish green reaction. The latter reaction accounts for the higher manganese levels recorded. The pearls emitted medium to strong yellowish green fluorescence under long-wave ultraviolet light and a similar weaker reaction under short-wave UV. Based on these analyses, a saltwater origin was confirmed for all of the pearls.

Examined with real-time X-ray microradiography (RTX), most of the pearls showed minimal growth arcs, and some revealed faint linear-looking features visible only in certain directions. External and internal features aroused suspicion that these pearls were NBC. Another important observation was related to the size and length of the drill holes. Given the importance of maintaining weight, it is customary to drill drop and oval pearls to approximately one-third of their length. These pearls, however, were drilled to a depth that covered more than two-thirds of

their length, while others were fully drilled with oversized drill holes. This indicated the pearls were drilled with the specific intention of concealing internal structures (Summer 2023 Lab Notes, pp. 218–220).

RTX imaging was performed for all the pearls in three directions, with careful alignment along their lengths to detect the presence of any linear feature or its remnants resulting from the drilling process. In most cases, proving a cultured origin only through RTX imaging was challenging. Consequently, the structures were studied using X-ray computed microtomography (μ -CT) analysis, as shown in table 1. In pearls 1 and 2, both undrilled, RTX imaging revealed a few distinct growth arcs, but not much was visible at their centers. Pearl 1 exhibited a small suspicious linear feature along its length, while pearl 2 did not. Interestingly, μ -CT analysis revealed an elongated linear feature running along the length of both pearls, accompanied by a few growth arcs, with the outer nacre lacking many growth features.

Pearls 3 and 4 were partially drilled, and both exhibited drill holes of unusual length and size compared to those observed in natural pearls. RTX imaging showed a few growth arcs toward the outer nacre and minimal growth at the center around the drill hole area. When aligned along their lengths, remnants of a linear feature crossing the drill hole were clearly visible in pearl 3, whereas pearl 4 did not show any evidence of the linear feature. Similarly, μ -CT analysis on both pearls revealed remnants of the linear feature toward the end of their drill holes, indicating an unsuccessful attempt to remove the linear features. Pearl 5, which was fully drilled, had fine growth arcs along its



Figure 12. Lot of 40 drop and oval pearls, with the smallest weighing 0.62 ct and measuring 5.17×4.16 mm and the largest weighing 2.95 ct and measuring 9.53×6.65 mm. Photo by Gaurav Bera.

TABLE 1. Surface appearance and internal structures of the pearl samples.

Sample	Macro	RTX	μ -CT
Pearl 1 1.44 ct 6.98 × 5.28 mm			
Pearl 2 1.79 ct 6.66 × 6.00 mm			
Pearl 3 1.70 ct 9.27 × 6.49 mm			
Pearl 4 2.04 ct 7.53 × 6.21 mm			
Pearl 5 1.43 ct 7.79 × 6.26 mm			

shape in RTX imaging, with a faint shadow feature running parallel to the drill hole. Through μ -CT analysis, a linear feature near the drill hole area was clearly visible.

As observed, structures from the samples closely resembled those observed in South Sea NBC pearls from the *Pinctada maxima* mollusk (A. Homkrajae et al., "Internal structures of known *Pinctada maxima* pearls: Cultured pearls from operated marine mollusks," Fall 2021 *G&G*, pp. 186–205). In particular, drop and oval pearls from this mollusk should be carefully examined to avoid misidentification as natural due to the absence of structure if only examined under RTX imaging.

Natural drop and oval pearls are highly valued, and those with exceptional appearance and size are not easy to find. In recent decades, some members of the trade have attempted to conceal the linear features visible in South Sea keshi pearls using film or dental X-ray machines and subsequent drilling to remove any evidence. This often results in remnants of the linear features being left behind, as observed in these samples. These remnants can only be identified by carefully aligning the pearls in RTX imaging and through μ -CT analysis. Such subtle features can be easily overlooked during testing, potentially leading to their misinterpretation and misidentification as natural pearls.

It is therefore essential for the trade to remain alert and informed about these increasingly frequent practices.

Roxane Bhot Jain, Abeer Al-Alawi, Anukul Belanke,
and Lubna Sahani
GIA, Mumbai

Two pen pearls from Bahrain. Pen or pinna pearls, also known as the “fan clam,” originate from the marine bivalve mollusk belonging to the genus *Pinna* or *Atrina*. They are commonly found across the Indo-West Pacific region, from southeastern Africa to Melanesia and New Zealand, extending north to Japan and south to New South Wales. Additionally, they can be found in the Mediterranean Sea, the Red Sea, and the Arabian (Persian) Gulf. Typically, the shell size ranges from 10 to 60 cm, producing pearls measuring up to 11 mm and rarely even 16 mm. Most of these pearls are non-nacreous, displaying colors ranging from yellowish orange to brown and black, while the nacreous pearls exhibit a silvery surface (*CIBJO Guide for Classifying Natural Pearls and Cultured Pearls*, 2021).

GIA’s Mumbai laboratory recently received two pen pearls for scientific examination. They were recovered by a renowned Bahraini diver from the shallow waters off Bahrain, fished at a depth of 2 meters in October 2023. Pearl A was a bicolor yellowish brown and black button shape, weighing 0.65 ct and measuring 4.65×4.25 mm, while pearl B was a yellowish brown near-button, weighing 0.73 ct and measuring 4.86×4.34 mm (figure 13). Visual



Figure 13. Two pen pearls from Bahrain displayed on a pen shell originating from the same waters. Both the shell and the pearls exhibit a similar color pattern. Pearl A measures 4.65×4.25 mm and weighs 0.65 ct (left); Pearl B measures 4.86×4.34 mm and weighs 0.73 ct (right). Photo by Gaurav Bera.

observation showed significant surface-reaching cracks on pearl A (figure 14A) and a network of crazing or cracking due to the columnar structure on pearl B (figure 14C). When viewed under 40 \times magnification with a fiber-optic light, both exhibited a translucent non-nacreous surface with a columnar calcite structure, displaying a pseudo-hexagonal cellular outline (N. Sturman et al., “Observations on pearls reportedly from the Pinnidae family (pen pearls),” Fall 2014 *G&G*, pp. 202–215).

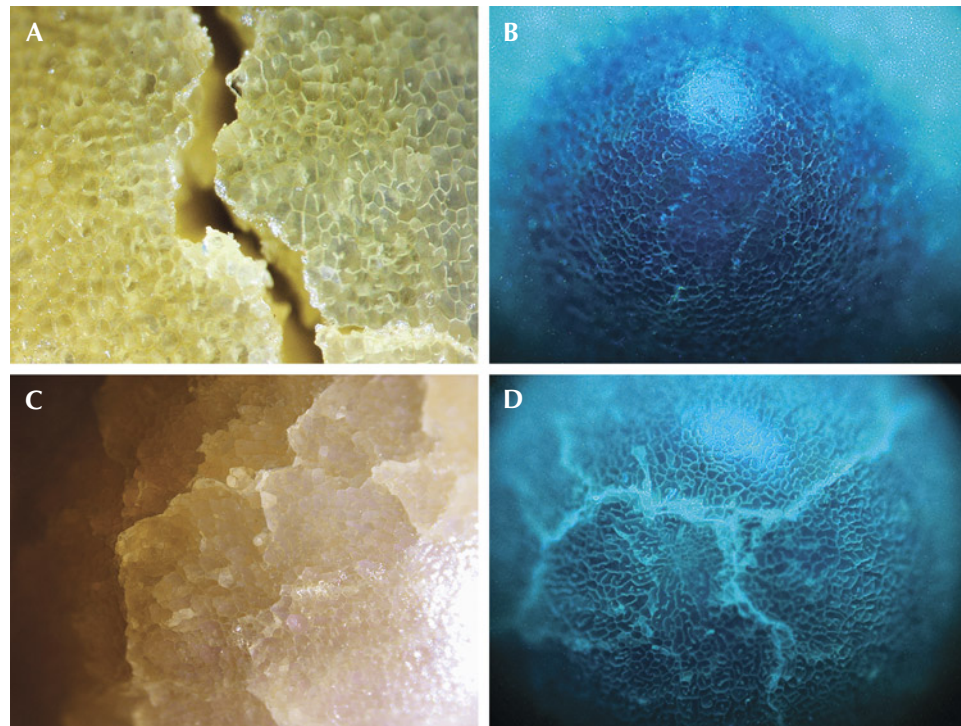


Figure 14. A: Non-nacreous cellular structure with a significant surface-reaching crack in pearl A; field of view 0.5 mm. B: DiamondView image of the cellular structure on the black area on pearl A. C: Cellular structure with a network of subsurface cracking on pearl B; field of view 1.6 mm. D: DiamondView image of a spectacular greenish blue reaction of the cellular structure and the subsurface cracks on pearl B. Images by Karan Rajguru (A, B, and D) and Pfokreni Nipuni (C).

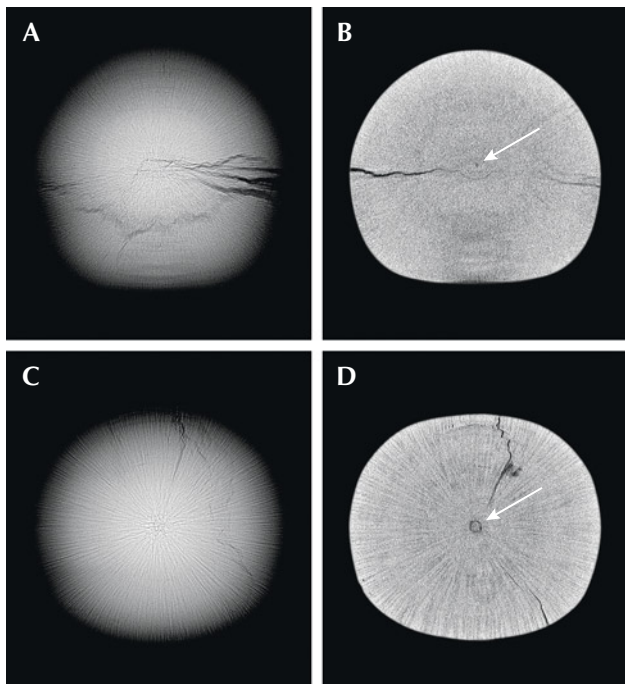


Figure 15. Top: RTX imaging of pearl A shows an acicular structure with significant surface-reaching cracks (A), and μ -CT imaging reveals a minute core (B). Bottom: RTX imaging of pearl B shows an acicular structure with a few subsurface cracks (C), and μ -CT imaging reveals a small central core (D).

The pearls showed an inert reaction when exposed to X-ray fluorescence. Energy-dispersive X-ray fluorescence spectrometry on both revealed manganese levels below detection limits and 45 ppm and higher strontium levels of 1183 ppm and 1303 ppm, respectively, confirming their saltwater origin. Under long-wave ultraviolet radiation, the black area on pearl A was inert, while the yellowish brown area showed a moderate yellowish green reaction similar to that of pearl B. Faint patchy reddish areas were also observed under the translucent surface of pearl B, a reaction linked to a type of porphyrin pigment. When exposed to

short-wave UV, pearl A was almost inert and pearl B showed a weaker yellowish green reaction. When examined by the deep-UV wavelength (<230 nm) of the DiamondView, both revealed a greenish blue reaction with a mosaic of fine cellular features of the columnar calcite structure (figure 14, B and D).

Real-time X-ray microradiography (RTX) and X-ray computed microtomography (μ -CT) were conducted to study the internal structures. RTX imaging of pearl A revealed a fine acicular (radial) structure with significant surface-reaching cracks (figure 15A). A minute core was visible in μ -CT imaging (figure 15B). Pearl B also exhibited an acicular structure but with broader radiating lines than those observed in pearl A (figure 15C). Similarly, μ -CT imaging revealed a small central core with a few minor cracks (figure 15D). These structures corresponded with the columnar structure observed on their surfaces (Fall 2009 GNI, pp. 69–71).

Raman spectroscopy using 514 and 830 nm laser excitation revealed peaks for both pearls at 280 and 712 cm^{-1} as well as 1085 cm^{-1} , indicative of calcite. The surface of pearl B was ground down, exposing a dark brown ring along with the acicular structure (figure 16, left). This ring was not visible in RTX or μ -CT imaging. Raman analysis on different spots of the ground pearl showed similar calcite peaks with a weak polyenic pigment peak at around 1437 cm^{-1} . Photoluminescence analysis for both pearls revealed very weak bands at 620, 650, and 680 nm , indicating natural coloration. These bands were more distinct on the cross-sectional areas of pearl B. In addition, the dark brown central core and ring exhibited a brownish red reaction when viewed under long-wave UV radiation (figure 16, right), linked to a type of porphyrin pigment previously recorded in partially non-nacreous and nacreous pearls from the *Pteria* species (S. Karampelas and H. Abdulla, “Black non-nacreous natural pearls from *Pteria* sp.,” *Journal of Gemmology*, Vol. 35, No. 7, 2017, pp. 590–592) and in a *Pinctada radiata* shell with a partially non-nacreous blister pearl (Winter 2023 GNI, pp. 527–529).

Non-nacreous pen pearls are often priced lower than their nacreous counterparts from the *Pinctada* species,

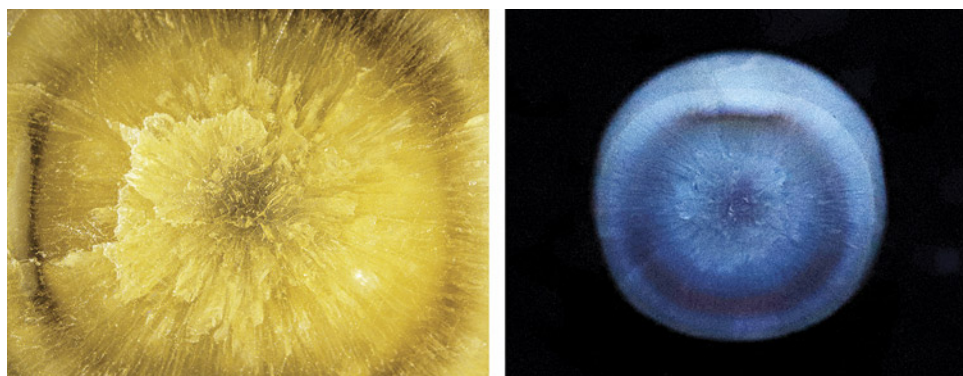


Figure 16. Left: Cross section of pearl B after grinding, revealing an acicular structure with a dark inner ring and a small central core; field of view 2.1 mm. Right: Long-wave UV image of the cross section with the dark ring and core showing a brownish red reaction. Photos by Karan Rajguru.



Figure 17. A rare 7.38 ct orangy red rhodonite. Photo by Chunyan Wang.

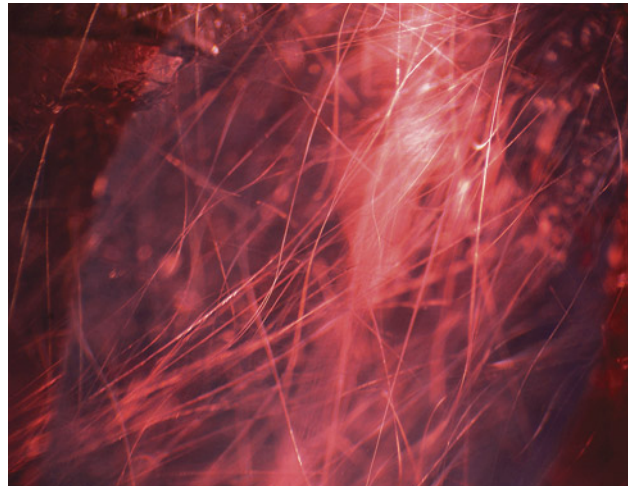


Figure 18. Many long tube inclusions were observed in the rhodonite sample. Photomicrograph by Chunyan Wang; field of view 2.36 mm.

mainly due to their durability issues related to surface cracks. Although not desirable for jewelry purposes, they have been used as nuclei for producing atypical bead cultured pearls. In such cases, identification becomes very challenging due to their internal structure composed of natural acicular growth features. This submission provided an interesting opportunity to study these known pen pearl samples from Bahrain, a habitat shared with the popular *Pinctada radiata* mollusk species.

Abeer Al-Alawi, Karan Rajguru, Pfokreni Nipuni, and Roxane Bhot Jain
GIA, Mumbai

Cummingtonite needles encased by quartz in a rhodonite. Recently, the authors examined a 7.38 ct gem-quality rhodonite exhibiting a vivid orangy red color and good transparency (figure 17). Gemological testing, Fourier-transform infrared spectroscopy, and Raman spectroscopy identified it as rhodonite. This gemstone had a refractive index of 1.733–1.747 and specific gravity of 3.46. Most rhodonite is opaque and is used as an ornamental stone, and transparent facet-grade material is very rare. Microscopic observation revealed an abundance of long, curved needles scattered randomly throughout the gem host (figure 18), consistent with previous studies. Occasional fluid inclusions were also seen.

A previous publication suggests that these curved needles are cummingtonite, an amphibole group mineral with a chemical formula of $(Mg, Fe^{2+})_2[Mg, Fe^{2+}]_5Si_8O_{22}(OH)_2$ (P. Leverett et al., "Ca-Mg-Fe-rich rhodonite from the Morro da Mina mine, Conselheiro Lafaiete, Minas Gerais, Brazil," *Mineralogical Record*, Vol. 39, 2008, pp. 125–130). Raman spectroscopy confirmed the identity of one needle as cum-

mingtonite, displaying characteristic peaks at 190, 667, and 1036 cm^{-1} when the laser beam was focused on the center of it. However, several new peaks appeared when the laser beam moved to the boundary between the needle and the rhodonite, including a 208 cm^{-1} peak that matched with quartz. Such a finding is new to the authors, since needle inclusions encased in another mineral have rarely been reported. To further investigate this finding, more than 10 points were selected, and the results identified quartz between the cummingtonite needle and the rhodonite host. All the tested Raman spectra were compared to the Raman online database.

To further explore the relationship between rhodonite, quartz, and cummingtonite needles, a 3D Raman map was performed on a selected area of $3 \times 14 \times 12 \mu\text{m}$ with a step size of $2 \mu\text{m}$. After running for 17.25 hours, more than 500 spectra were recorded. Three feature peaks were selected for image reconstruction: 3658 cm^{-1} for cummingtonite, 113 cm^{-1} for rhodonite, and 208 cm^{-1} for quartz (figure 19). Due to the similarity between the Raman spectra of cummingtonite and rhodonite, the main peaks were not chosen for mapping. The OH-related peak at 3658 cm^{-1} was only observed in cummingtonite, enabling us to distinguish the two minerals. The Raman mapping image is shown in figure 20, with blue indicating the host, green for quartz, and red for cummingtonite. These images revealed that the detection of quartz between rhodonite and cummingtonite was not by accident but indicated a considerable presence of quartz inclusions. Previous studies have reported quartz as an isolated and random mineral inclusion in rhodonite from Australia (e.g., P. Millsteed et al., "Inclusions in transparent gem rhodonite from Broken Hill, New South Wales, Australia," Fall 2005 *G&G*, pp. 246–254). Based on our observation of the position of the

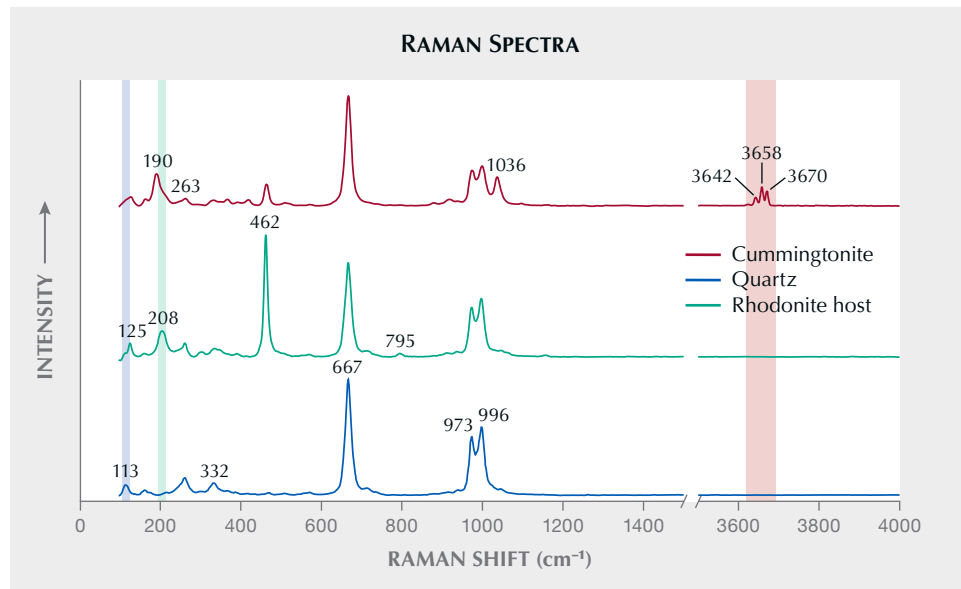


Figure 19. The Raman spectra of cummingtonite, quartz, and rhodonite. While the long tube was identified as cummingtonite, quartz was detected between the tube and the rhodonite host. Spectra are offset vertically for clarity.

quartz, we speculate that it may be the product of the decomposition of cummingtonite under certain temperatures and pressures.

This intricate inclusion association pattern may offer a new perspective on the origin of curved needles in rhodonite. This case also highlights the usefulness of Raman mapping as a tool for nondestructive analysis of inclusions.

Yujie Gao, Xueying Sun (shirley.sun@guildgemlab.com), and Ziyun Zhang

Guild Gem Laboratories, Shenzhen, China

*Ruobin Tang
Chengdu, China*

Update on Liberian ruby. Liberian rubies were reported more than a decade ago (L. Kiefert and M. Douman, "Ruby from Liberia," Summer 2011 *G&G*, p. 138). These rubies were found in two diamond mines located along the Mano River and in Nimba Province close to the Guinean border. GIA's Tokyo laboratory recently received 10 Liberian corundum samples (figure 21) from the Japan-based NGO Diamonds for Peace. These samples were collected at Weasua, Liberia, the same locality recently reported in *G&G* (Spring 2023 GNI, pp. 149–150).

Most of the rough corundum pebbles recovered from Weasua showed weakly saturated purplish red, pink, pale yellow, and green colors; most fall in the color range of sapphire, except for a few red ones. Three of the ruby sam-

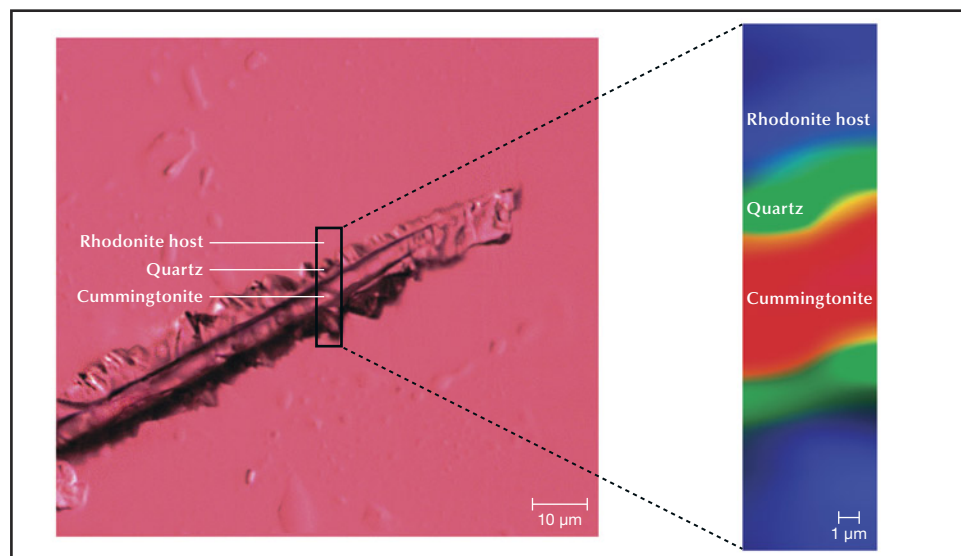


Figure 20. 3D false-color Raman mapping of one of the encased needle inclusions with the surrounding host. The rectangle shows the mapping area. The blue area indicates the existence of the rhodonite host, the green area the quartz, and the red area indicates the cummingtonite.

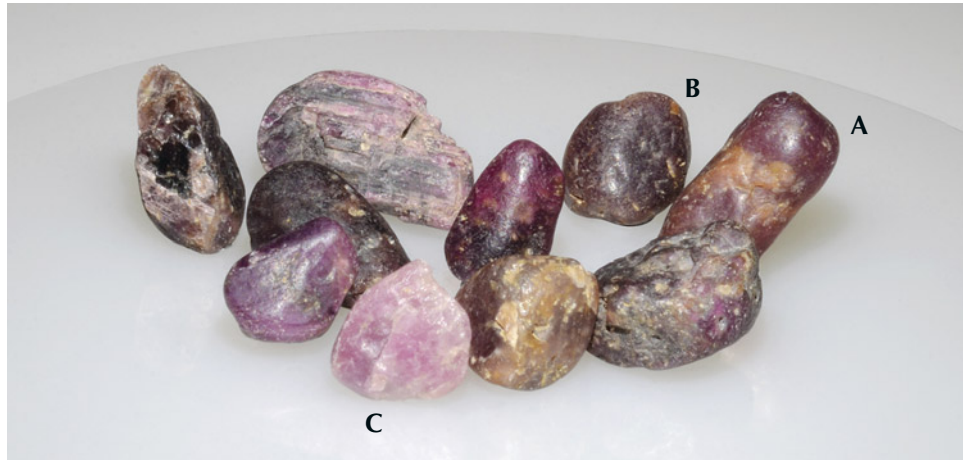


Figure 21. Ten corundum samples from the Lofa River in Weasua, Liberia. Photo by Shunsuke Nagai.

ples—11.65 ct purplish red (A), 6.52 ct dark purplish red (B), and 5.37 ct light purplish red (C)—were cut and polished for observation and advanced testing. Standard gemological testing yielded a refractive index of 1.762–1.770, a uniaxial interference pattern, and a hydrostatic specific gravity of 3.85–3.99. Except for the specific gravity, which is slightly low presumably due to the inclusions, the gemo-

logical characteristics were consistent with corundum.

The rounded surfaces of the rough stones suggested weathering. Most were semitransparent to translucent, heavily included, and displayed lamellar twinning structures in two orientations (figure 22). The twinning planes were filled with orange secondary minerals. Other internal features included irregularly shaped reflective particles

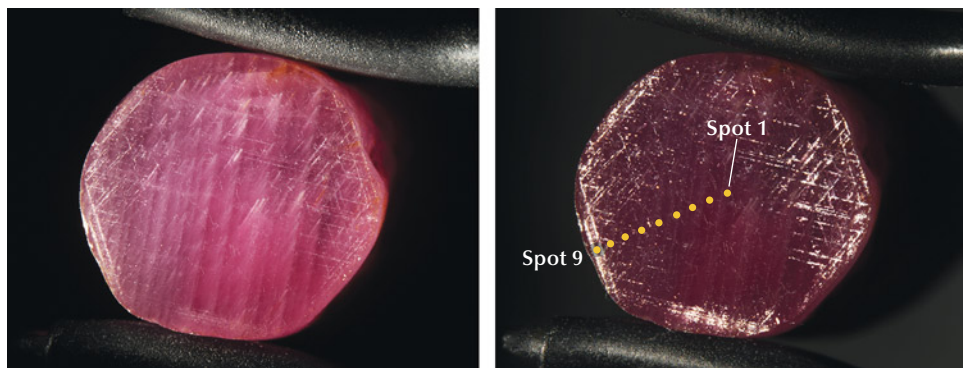


Figure 22. Sample A shows strong two-direction lamellar twinning structures (top left) and contains numerous reflective inclusions near the rim (top right). Both photos are under fiber-optic illumination; the light source of the top right photo is in a specific direction to show the reflective inclusions. Photomicrographs by Yuxiao Li; field of view 19.5 mm. The plot at the bottom shows the minor/trace element concentrations of each spot. The spot position is shown in the top right photo.

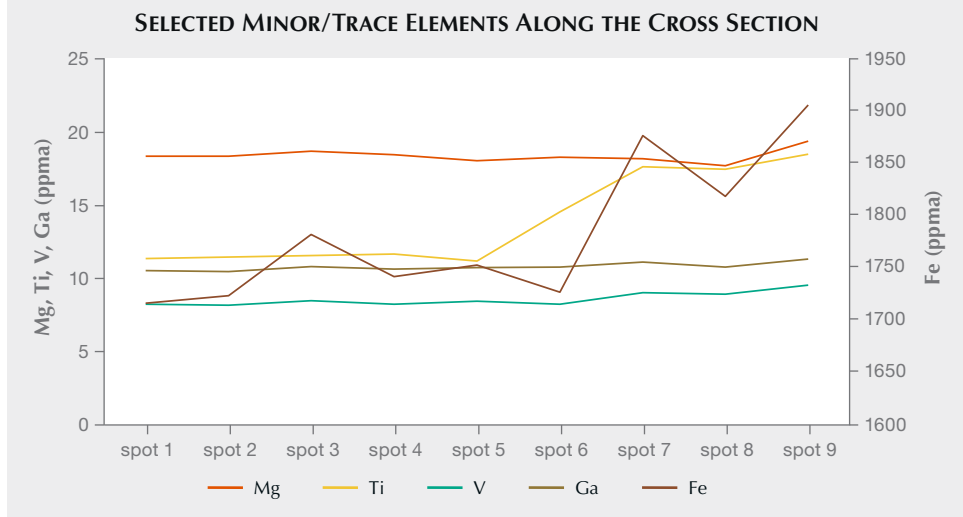


TABLE 1. Minor and trace element concentrations (in ppma) of rubies from Liberia.

	Mg	Ti	V	Fe	Ga
Sample A	17.70–19.38	11.2–18.5	8.17–9.57	1716–1906	10.47–11.32
Sample B	14.78–21.14	21.4–28.8	16.25–16.53	1340–1347	24.39–25.77
Sample C	21.39–25.51	23.3–84.4	4.36–5.20	968–997	8.80–9.62
Total	14.78–25.51	11.2–84.4	4.36–16.53	968–1906	8.80–25.77
Detection limit (ppma)	0.04	0.1	0.01	2	0.01

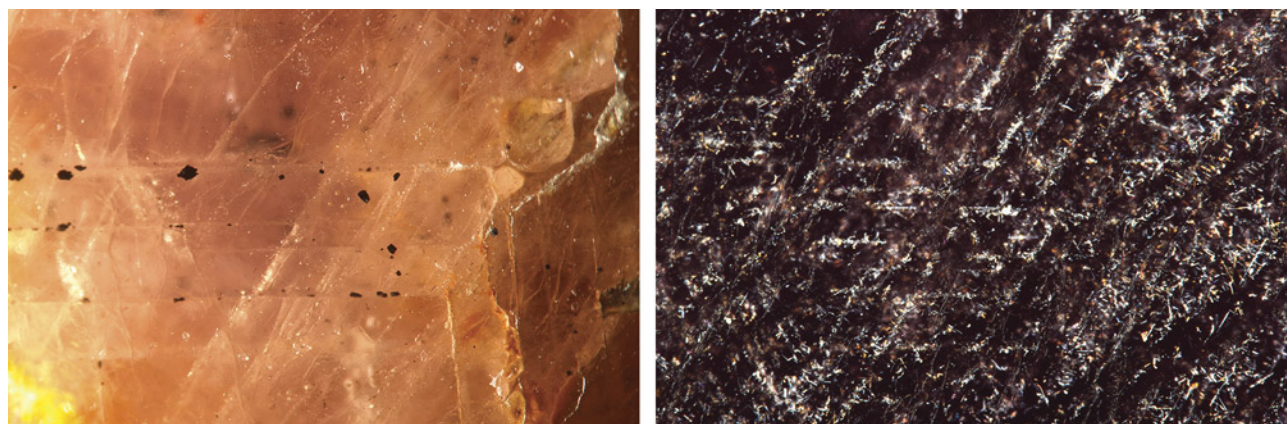
aligned in three directions, iridescent small particles, and fine needles (figure 23). Sample A showed a less-included core and particle-rich rim, and sample B was heavily included with large whitish aggregate inclusions and some small black minerals along the twinning planes. These black minerals were identified by Raman spectroscopy as vonsenite ($\text{Fe}^{2+},\text{Fe}^{3+}[\text{BO}_3]\text{O}_2$).

Laser ablation-inductively coupled plasma-mass spectrometry (LA-ICP-MS) was carried out to analyze trace element compositions. On sample A, we measured nine spots from center to edge. The rim area (spots 7–9) yielded higher iron and titanium, and similar levels of magnesium, vanadium, and gallium compared with the less-included core area (spots 1–6) (figure 22). We measured three spots on each of the remaining two samples. The results are pre-

sented in table 1, showing the wide range of concentrations of titanium, vanadium, iron, and gallium. (Spot 1 of sample B shows high titanium (84.3 ppma) with zirconium (0.054 ppma), likely caused by the contamination of small inclusions.)

Kongsomart et al. (Winter 2017 GNI, pp. 472–473) summarized the trace element concentrations in rubies from East African deposits. Samples A and C of the Liberian rubies in this study showed trace element concentrations similar to those from Mozambique. Sample B had a high gallium concentration, overlapping with rubies from the Zahamena deposit in Madagascar. Considering the wide range of trace element concentrations of Liberian rubies and those from East African deposits, these chemistry components are not helpful in separating the Liberian ruby

Figure 23. Black inclusions, identified as vonsenite by Raman spectroscopy, were observed with twinning planes (left) and reflective particles aligned in three directions with fine needles (right). Photomicrographs by Yuxiao Li; fields of view 2.4 mm (left) and 2.9 mm (right).



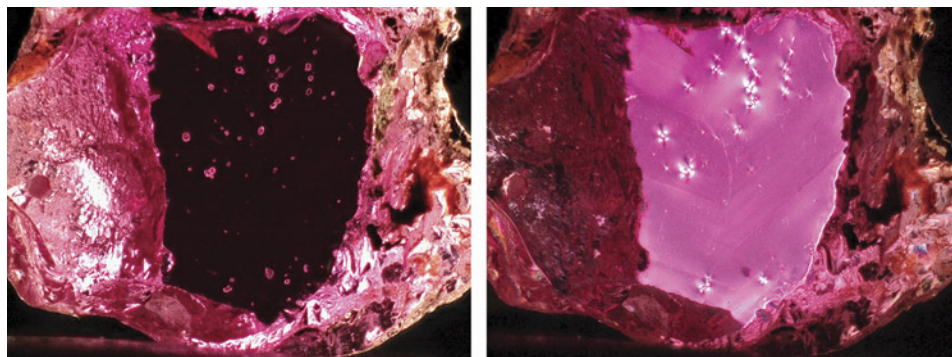


Figure 24. Colorless crystals with high relief (left) in a ruby mined near Caraia in the Montepuez region. Placing the ruby between crossed polarizers (right) revealed a stress halo caused by low-dose radiation emitted by the zircon inclusion. Photomicrographs by Wim Vertriest; field of view 3.6 mm.

from other origins. The ruby samples from these East African origins are less included than the Liberian samples in this study. For identification services, we are able to determine the origin not only by trace elements but also by microscopic observations (A.C. Palke et al., "Geographic origin determination of ruby," Winter 2019 *G&G*, pp. 580–613). If it is necessary to separate Liberian rubies from other highly included low-quality rubies, comprehensive study on such included samples is needed.

Recently, some low-quality rubies reportedly mined from Guinea have been sold on the market. These materials are often heat treated and filled with lead glass, with some cabochons displaying six-rayed asterism after treatment. Both rough samples of Guinean ruby in the GIA colored stone reference collection and the studied Liberian rubies show a classic weathered "barrel" shape, semitransparent to translucent transparency, pinkish color, and most are heavily included. Given that the deposit of Guinea ruby is located upstream, north of Liberia, these rubies presumably originated from the same or closely related geological condition. With proper treatment, Liberian rubies could show asterism and be used as jewelry material.

*Yuxiao Li and Yusuke Katsurada
GIA, Tokyo*

*Chie Murakami and Mai Suzuki
Diamonds for Peace, Yokohama*

Update on inclusion scenes in Mozambican rubies. In August 2022, a team of GIA gemologists visited the ruby mines near Montepuez in the Cabo Delgado province of northern Mozambique (Fall 2022 GNI, pp. 383–386). This included a visit to the deposits farther west in the region, near the village of Caraia. This mining area is north of the N14 road, while most of the previously known productive ruby deposits are southeast of this highway.

Ruby mining near Caraia has been ongoing for more than a decade but was mostly limited to artisanal mining activity until 2017. In the last few years, the ruby deposits have been developed on a larger scale by Fura Gems. The first official sale of this material took place in late 2021, and regular auctions have been organized since then (Fall 2021 GNI, pp. 276–277).

During GIA's visit in August 2022, gemologists collected a large suite of rough rubies directly from the wash plant and sort house at the mine site. The samples ranged from 0.1 to 1.2 g and were transparent and fracture-free. The vast majority contained some crystal inclusions, and an extensive inclusion study of this material matched well with the known data from Mozambican ruby, with one exception. The most common inclusions are bands of fine silk, short needles, and particles, including reflective platelets. Mozambican rubies typically show three distinctive types of solid crystals: transparent greenish amphibole crystals with a stubby to elongated shape; pseudohexagonal frosty mica crystals with small expansion fractures; and black opaque sulfide crystals with a metallic luster. All of these features were prevalent in the rubies mined near Caraia.

However, one observation stood out: In 8 of the 85 studied samples, zircon crystal inclusions were found. While zircon crystals are also transparent, their relief is higher than that of the more common amphibole crystals. They also tend to be smaller and are rarely elongated in rubies. The most efficient way to identify them is by viewing the stones between crossed polarizers, which highlights the obvious stress halos around the slightly radioactive zircon crystals (figure 24). In all of GIA's samples, the identification was also confirmed by confocal Raman spectroscopy.

To our knowledge, zircon crystals have not been previously documented in rubies from Mozambique. They are, however, a hallmark for rubies from Madagascar (A.C. Palke et al., "Geographic origin determination of ruby," Winter 2019 *G&G*, pp. 580–612). The presence of zircon crystal inclusions is often a decisive discriminator in the origin determination of rubies. The inclusion scenes of high-quality Mozambican and Malagasy rubies can look very similar, but only the latter were known to have abundant zircon inclusions. This is no longer true now that zircon inclusions have also been identified in rubies from Mozambique.

Trace element analysis can often assist in separating rubies from East African sources. But even there, some overlap occurs between Mozambique and Madagascar, especially for stones with higher iron concentrations. All the Mozambican rubies with zircon inclusions showed a trace element signature that matched completely with other Mozambican rubies when analyzed with both energy-dis-

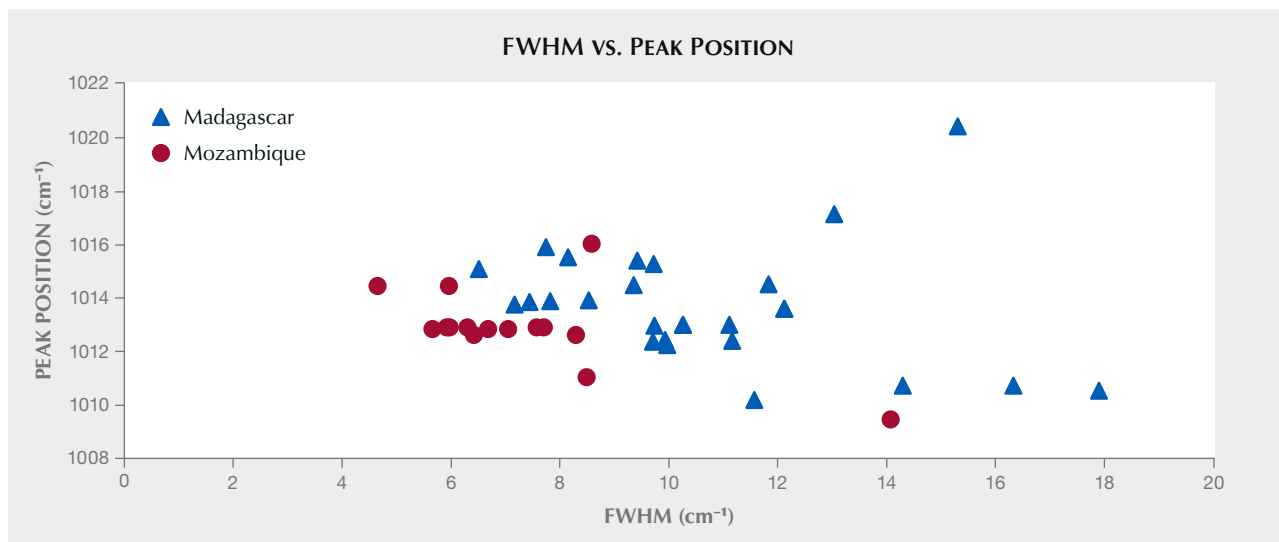


Figure 25. This chart shows the FWHM vs. the peak position of the most important peak (1015 cm^{-1}) in the Raman spectrum of zircon inclusions in Mozambican and Malagasy rubies.

persive X-ray fluorescence and laser ablation–inductively coupled plasma–mass spectrometry. Fortunately, the rubies from Caraia tend to have a low iron concentration, reducing the likelihood that their trace chemistry composition will match with Malagasy rubies, which tend to have higher iron concentrations.

Raman spectra of the zircons in rubies from Mozambique (15 inclusions in 6 different stones) and Madagascar (27 inclusions in 13 different stones) showed that the main peak (1015 cm^{-1}) in Mozambican zircon inclusions tends to have lower full width at half maximum (FWHM), but there is no clear separation between the two populations based on the Raman spectra of the zircon inclusions (figure 25).

The discovery of zircon inclusions in Mozambican rubies has a potentially major impact on the origin determination criteria used for the two most common sources of East African ruby. These new discoveries also highlight two important aspects of origin determination research: the critical need to keep collecting samples from known deposits to identify new features in current production, and the power of the microscope as an identification tool in a gemological laboratory.

Wim Verriest

ANNOUNCEMENTS

William Ruser: The Jeweler Who Charmed Hollywood. A new book by Judy Colbert and Peggy Tsiamis chronicles the life of “Jeweler to the Stars” William Ruser, best known for his whimsical figural jewelry with freshwater pearls. Ruser’s celebrity clientele included Frank Sinatra, Elizabeth Taylor, Joan Crawford, and Ronald Reagan during Hollywood’s golden age. With little published about Ruser, the research and interviews conducted for the book reveal personal and professional details about the jeweler and his

business on Rodeo Drive in Beverly Hills. The book (figure 26) also features more than 100 images. *William Ruser: The Jeweler Who Charmed Hollywood* is available through the GIA store (<https://store.gia.edu/collections/history-lore>).

Figure 26. Jeweler William Ruser owned a prestigious store on Rodeo Drive in Beverly Hills during Hollywood’s golden age.

